Landscape Change Affects Soil Organic Carbon Mineralization and Greenhouse Gas Production in Coastal Wetlands

Ping Yang[1,2,3*], Linhai Zhang[1,2,3], Derrick Y. F. Lai[4], Hong Yang[5,6], Lishan Tan[7], Liangjuan Luo[1,2], Chuan Tong[1,2,3*], Yan Hong[1], Wanyi Zhu[1,2], Kam W. Tang[8*]

[1]School of Geographical Sciences, Fujian Normal University, Fuzhou, P.R. China,

[2]Key Laboratory of Humid Subtropical Eco-geographical Process of Ministry of Education, Fujian Normal University, Fuzhou, P.R. China

[3]Research Centre of Wetlands in Subtropical Region, Fujian Normal University, Fuzhou, P.R. China

[4]Department of Geography and Resource Management, The Chinese University of Hong Kong, Shatin, New Territories, Hong Kong SAR, China

[5]College of Environmental Science and Engineering, Fujian Normal University, Fuzhou, China

[6]Department of Geography and Environmental Science, University of Reading, Reading, U.K.

[7]State Key Laboratory of Estuarine and Coastal Research, East China Normal University, Shanghai, China

[8]Department of Biosciences, Swansea University, Swansea, U.K.

***Correspondence to:**

Ping Yang (yangping528@sina.cn); Chuan Tong (tongch@fjnu.edu.cn); Kam W. Tang (k.w.tang@swansea.ac.uk)

Abstract

Plant invasion and aquaculture activities have drastically modified the landscape of coastal wetlands in many countries, but their impacts on soil organic carbon (SOC) mineralization and greenhouse gas production remain poorly understood. We measured SOC mineralization rate and soil CO_2 and CH_4 production rates in three habitat types from 21 coastal sites across the tropical and subtropical zones in China: native mudflats (MFs), *Spartina alterniflora* marshes (SAs) and aquaculture ponds (APs). Landscape change from MFs to SAs or APs increased total and labile fraction of SOC, as well as carbon mineralization rate and greenhouse gas production, but there were no discernible differences in SOC source-sink dynamics between SAs and APs. SOC mineralization rate was highest in SAs (20.4 μg g^{-1} d^{-1}), followed by APs (16.9 μg g^{-1} d^{-1}) and MFs (11.9 μg g^{-1} d^{-1}), with CO_2 as the dominant by-product. Bioavailable SOC was less than 2% and was turned over within 60 days in all three habitat types. Proliferation of *S. alterniflora* marshes and expansion of aquaculture pond construction had resulted in a net increase in soil CO_2-eq production of 0.4–4.3 Tg yr^{-1} in the last three decades. Future studies will benefit from better census and monitoring of coastal habitats in China, complementary *in situ* measurements of greenhouse gas emissions, and more sampling in the southern provinces to improve spatial resolution.

Plain Language Summary Wetlands are one of the largest reservoirs of soil carbon and play importance role in the global terrestrial biogenic carbon cycle. Coastal wetlands are major sinks for carbon due to high sedimentation rate and burial of organic matter. However, landscape modifications due to invasive vegetation and aquaculture activities have profoundly impacted the carbon source-sink dynamics in coastal wetlands. We compared the soil organic carbon turnover and greenhouse gas (CO_2 and CH_4) production between native mudflat, *Spartina* marshes and aquaculture ponds in five coastal provinces across the tropical-subtropical gradient in China. Landscape modification of native mudflats increased soil carbon mineralization rate and greenhouse gas production, predominantly as CO_2, and the effect was consistent across the large geographical and climate gradients. Our results provide a better insight into the carbon dynamics in impacted wetlands across a large geographical range.

List of abbreviations:

APs: Aquaculture ponds

BD: Soil Bulk Density

CO_2: Carbon Dioxide

CH_4: Methane

C_0: Bioavailable SOC

DOC: Dissolved Organic Carbon

DON: Dissolved Organic Nitrogen

EF: Environmental Factors

MBC: Microbial Biomass Carbon

MFs: Mud flat

MBN: Microbial Biomass Nitrogen

SAs: *Spartina alterniflora* marshes

Sal: Soil Salinity

SOCM: SOC Mineralization Rate

SOC: Soil Organic Carbon

Soil C:N: Total Carbon: Total Nitrogen

ΣSOCM: Cumulative anaerobic SOC Mineralization

s(RR_{++}): Standard error of RR_{++}

SPS: Soil Particle Size

SWC: Soil Water Content

RR: Response Ratio

RR_{++}: Weighted Response Ratio

TC: Total Carbon

TN: Total Nitrogen

1. Introduction

Wetlands are considered to be among the most productive but vulnerable ecosystems (Kirwan & Megonigal, 2013; Su et al., 2021; Wen et al., 2019). Despite covering just 4–6 % of the total land area, wetlands hold approximately 450 Pg of the global soil carbon, representing 25–30 % of the terrestrial biosphere carbon pool (Kayranli et al., 2010). Coastal wetlands are a crucial sink in the global carbon cycle due to high sedimentation rate and burial of organic matter (Drake et al., 2015; Packalen et al., 2014; Zhang et al., 2021a), and it is estimated that coastal wetlands globally store at least 53.7 Tg C yr^{-1} (Wang et al., 2021). However, wetland habitats have been impacted around the world, and despite international initiative to protect these habitats (e.g. Ramsar Convention on Wetlands), wetland degradation and loss rate remains high in Asia (Davidson, 2014), potentially altering the land's carbon source-sink dynamics over different time and spatial scales (Mitsch et al., 2013).

Plant invasion and land-use change are two major threats to the world's coastal wetlands (Sun et al., 2015; Walker and Smith 1997; Zhu et al., 2020). Invasive plant species may alter the soil microbial community compositions and dynamics, above- and below-ground carbon pools, primary productivity, and nutrient and carbon mineralization rates (Piper et al., 2015; Yuan et al., 2019; Zhang et al., 2010). Land-use change can modify hydrology, nutrient cycles, soil properties and overall ecosystem structure (Andreetta et al., 2016; Dick & Osunkoya, 2000; Gao et al., 2019). Increasing range shift by exotic species and coastal development will intensify these threats, potentially changing the dynamics of soil organic carbon (SOC) and subsequent production of greenhouse gases such as carbon dioxide (CO_2) and methane (CH_4) (Gao et al., 2018a; Yang et al., 2017), and their feedback effect on climate is a major concern.

China accounts for about 4.2% of the global wetland area, and despite the conservation effort, wetlands still disappear at a rate close to 1% per year (Meng et al., 2017). Coastal wetlands in mainland China cover an estimated area of 5.79 M ha across its southern and eastern seaboards, and invasion by *Spartina alterniflora* and land-use change for aquaculture have profoundly changed this coastal landscape (Duan et al., 2020; Ren et al., 2019; Sun et al., 2015). For example, *S. alterniflora* was first introduced into China in 1982 and by 2015, *S. alterniflora* marshes had covered 54,600 ha (Mao et al., 2019). Similarly, it has been estimated that coastal aquaculture ponds in China grew from 6,000 km^2 to ~10,000 km^2 in the past three decades (Duan et al., 2021). To-date, most of the research has been focused on changes to wetland ecosystem at the local scale, in terms of SOC (Gao et al., 2016), soil composition (Wang et al., 2019) and stability (Yang et al., 2016; Zhang et al., 2021b) and related carbon emissions (Gao et al., 2018b; Tan et al., 2020; Yang et al., 2017), but they do not allow for a fuller comparison of the SOC and greenhouse gas dynamics in impacted coastal wetlands across the wider geographical and environmental gradients. There has been only one study that compared SOC and plant biomass compositions (C, N and P) from eight coastal locations invaded by *S. alterniflora*, but it did not examine greenhouse gas production (Wang et al., 2019). Also, many of the coastal wetland areas in China have been converted into aquaculture ponds, which were not included in the earlier study (Wang et al., 2019).

In order to generate a more comprehensive understanding of the biogeochemical consequences of habitat modification in coastal wetlands, we systematically studied 21 coastal wetland areas spanning 20°42′ N to 31°51′ N in mainland China. We hypothesized that soil organic carbon content and carbon mineralization rate would increase when mudflats were converted into marshes due to organic input from marsh vegetation, which could also lead to higher greenhouse gas production. We expected the soil properties to change in the opposite direction when marsh vegetation was removed to create aquaculture ponds. We further hypothesized that landscape modification dominated over other local environmental factors in affecting soil properties and greenhouse gas production across the broad latitudinal range.

To test these hypotheses, we sampled three habitat types at each location: native mudflats, mudflats that were converted into marshes by invasive *S. alterniflora*, and aquaculture ponds that were created from *S. alterniflora* marshes. We compared the soil physicochemical properties, SOC, carbon mineralization rate, and soil CO_2 and CH_4 production rates. The results will improve our understanding of the changes to soil characteristics in coastal wetlands as results of *S. alterniflora* invasion and aquaculture activities, the consequent carbon turnover and greenhouse gas production, and the related environmental drivers.

2. Methods

2.1. Study Area

Field sampling campaigns were conducted in five Chinese provinces including Shanghai (SH), Zhejiang (ZJ), Fujian (FJ), Guangdong (GD), and Guangxi (GX) (Figure 1). The large latitudinal and longitudinal ranges (20°42′ N to 31°51′ N; 109°11′ E to 122°11′ E) covered a tropical-to-subtropical climate gradient. The annual average temperature range was 11.0–23.0 °C and precipitation range was 1000–2200 mm across the five provinces. Their coastal wetlands combined cover about 2.58×10^6 ha, or 44.5 % of the total coastal wetlands in China (Sun et al., 2015), and they all have been impacted by *S. alterniflora* invasion or construction of aquaculture ponds. There was approximately 334 km^2 of *S. alterniflora* marshes (Liu et al., 2018) and 5309 km^2 of aquaculture ponds (Duan et al., 2020) along the coastal zone of the five provinces, representing 61.2% and 36.9% of the total areas of *S. alterniflora* marshes and aquaculture ponds, respectively, in China.

2.2. Soil Sampling

Field sampling was conducted in December 2019 and January 2020 at 21 sites across the five provinces, with two sites in SH, six in ZJ, nine in FJ, three in GD and one in GX (Figure 1). At each site, triplicate surface soil samples (top 20 cm) were collected from the three habitats (mud flat, *S. alterniflora* marshes and aquaculture ponds) using a steel corer (1.5 m length; 5 cm internal diameter) and transferred into ziplock bags; a total of 189 soil samples were collected (21 sampling sites × 3 habitats × 3 plots). All soil samples were transported in a chilled cooler to the laboratory, where they were stored at 4 °C until processing.

2.3. Analyses of Soil Physicochemical Properties.

In the laboratory, a subsample of the soil was freeze-dried, homogenized and then ground to a fine powder for measuring pH, salinity, soil particle size, inorganic nitrogen, Cl^-, SO_4^{2-}, total carbon (TC), total nitrogen (TN) and soil organic carbon (SOC). Soil pH was measured by an Orion 868 pH meter (Thermo Fisher Scientific, Cambridge, Massachusetts, USA; a 1:2.5 soil/distilled water mixture) with a measurement precision of ±1.0%. Soil salinity was measured by a Eutech Instruments-Salt6 salinity meter (Thermo Fisher Scientific, San Francisco, California, USA; a 1:5 soil/distilled water mixture) with a measurement precision of ±1.0%. A subsample was treated with the deflocculant hexametaphosphate and then analyzed for particle size based on laser diffraction (Mastersizer 2000, Malvern Instruments, Malvern, UK). Soil particle size (SPS) was calculated on a volume basis using the Malvern proprietary software. Soil inorganic nitrogen species (NH_4^+-N and NO_3^--N) were extracted by 2 M KCl (Gao et al., 2019; Yin et al., 2017) and quantified by a flow injection analyzer (Skalar Analytical SAN^{++}, Netherlands) (Yang et al., 2021). The detection limit and relative standard deviation (RSD) for inorganic nitrogen were 0.6 μg L^{-1} and ≦3.0% in 24 hr, respectively. Soil Cl^- and SO_4^{2-} contents were determined according to Chen & Sun (2020). Soil TC and TN were determined using a combustion analyzer (Elementar Vario MAX CN, ELEMENTAR, Hanau, Frankfurt, Germany) with a measurement precision of ±2.0%. Soil water content (SWC) and bulk density (BD) were determined after drying fresh soil at 105 °C for 48 h (Percival & Lindsay, 1997; Yin et al., 2019).

SOC was measured according to Liu et al. (2017). Briefly, 3 g of air-dried sample was screened, weighed and extracted in 1 M hydrochloric acid (HCl) solution for 24 h, then oven-dried at 60 °C. Afterward, SOC was determined by a combustion analyzer (Elementar Vario MAX CN, ELEMENTAR, Hanau, Frankfurt, Germany) based on standard procedures. The microbial biomass carbon (MBC) and nitrogen (MBN) contents were measured using the chloroform fumigation extraction method (Templer et al., 2003; Vance et al., 1987). Briefly, two portions of 10 g soil sample were fumigated with ethanol-free $CHCl_3$ for 24 h; two additional 10 g samples were not fumigated (Wang et al., 2011). All samples were then extracted in 0.5 M K_2SO_4 solution. Afterwards, the soil extracts were analyzed for total dissolved organic carbon (DOC) and total dissolved organic nitrogen (DON) using a TOC analyzer (Schimadzu TOC-$V_{CPH/CPN}$, Kyoto, Japan) with a measurement precision of ±2.0% and a flow injection analyzer (Skalar Analytical SAN^{++}, Netherlands) with a measurement precision of ±3.0%, respectively. Soil MBC and MBN contents were calculated from the differences in extractable DOC and DON between fumigated and unfumigated samples, using a K_{EC} (correction factor) of 0.38 for MBC and 0.54 for MBN (Li et al., 2010; Vance et al., 1987).

2.4. Soil Organic Carbon Mineralization Incubation Experiment

The rates of anaerobic mineralization of SOC into CO_2 and CH_4 were determined according to Kane et al. (2013) and Luo et al. (2019b). Briefly, approximately 30 g of fresh soil sample was put into a 200 mL glass incubation bottle (in triplicate); deoxygenated *in situ* water was then added in 1:1 v/v to make a slurry with 160 mL headspace. All incubation bottles were flushed with pure N_2 gas for 5–8 min to create an anoxic condition (Vizza et al., 2017; Wassmann et al., 1998), then sealed with a silicone rubber and incubated for 60 days at *in situ* temperature. On Days 1, 3, 7, 14, 21, 30, 45 and 60, each bottle was shaken on a rotary shaker for 0.5 h at 200 rpm min^{-1} to drive CO_2 and CH_4 into the headspace (Luo et al., 2019a); 5 mL of the headspace gas sample was then withdrawn with a syringe and 5 mL of pure N_2 gas was added back to maintain the pressure (Yang et al., 2019). The extracted gas samples were analyzed for CH_4 and CO_2 on a gas chromatograph equipped with a flame ionization detector (FID) (GC-2010, Shimadzu, Japan). Three CH_4 (or CO_2) gas standards, namely 1.96 (490.5), 8.25 (1003.4), and 100.3 (3090.3) ppm, were used in the calibration. The detection limits for CH_4 and CO_2 were 0.3 ppm and 1.0 ppm, respectively, and the measurement reproducibility was ≦2.0% and ≦3.0%, respectively. The measured CO_2 and CH_4 concentrations were corrected for pH, headspace volume, pressure and temperature (Ye et al., 2012), and was corrected for the dilution effect from the added N_2 gas (Tong et al., 2010). SOC mineralization rate [SOCM; μg C g^{-1} (dry weight) day^{-1}] was estimated from the combined CO_2 and CH_4 produced per gram of dry soil over time. Soil dry weight was calculated from the sample wet weight and its water content (see section 2.3). The cumulative mineralization of SOC over the 60 days of incubation (ΣSOCM) was fitted to a first-order kinetic equation to derive the mineralization rate constant (k; d^{-1}) (Cooper et al., 2011; Hyvonen et al., 2005):

$$\Sigma \mathrm{SOCM} = C_0 \times \left[1 - exp\left(-kt\right)\right] \qquad \text{Eq.(1)}$$

where ΣSOCM is the cumulative amount of CO_2–C and CH_4–C mineralized from SOC (μg C g^{-1}), C_0 is the initial bioavailable SOC (μg C g^{-1}), and t is the incubation time (d).

2.5. Calculation of ΔEF, ΔΣSOCM and ΔSOC Mineralization Parameters

To explore the synchronous responses of various environmental and soil parameters to habitat modification as results of plant invasion and aquaculture pond creation, we examined the rates of change of environmental factors (ΔEF), cumulative SOC mineralization (ΔΣSOCM), and SOC mineralization parameters [ΔC_0, Δk, and $\Delta(C_0/\mathrm{SOC})$], which were calculated as follows:

$$\Delta\mathrm{EF} = \frac{(\mathrm{EF_A} - \mathrm{EF_B})}{\mathrm{EF_B}} \qquad \text{Eq.(2)}$$

$$\Delta\Sigma\mathrm{SOCM} = \frac{(\Sigma\mathrm{SOCM_A} - \Sigma\mathrm{SOCM_B})}{\Sigma\mathrm{SOCM_B}} \qquad \text{Eq.(3)}$$

$$\Delta C_0 = \frac{C_{0\mathrm{A}} - C_{0\mathrm{B}}}{C_{0\mathrm{B}}} \qquad \text{Eq.(4)}$$

$$\Delta k = \frac{(k_\mathrm{A} - k_\mathrm{B})}{k_\mathrm{B}} \qquad \text{Eq.(5)}$$

$$\Delta(C_0 / SOC) = \frac{[(C_0 / SOC)_\mathrm{A} - (C_0 / SOC)_\mathrm{B}]}{(C_0 / SOC)_\mathrm{B}} \qquad \text{Eq.(6)}$$

where the subscripts B and A denote before and after habitat modification, respectively. The relationships between ΔΣSOCM (or ΔSOC mineralization parameters) and ΔEF were further examined to reveal the key EF affecting SOC mineralization in the different habitats.

2.6. Calculation of Response Ratio and Weighted Response Ratio

The response ratio (RR) was calculated to assess the responses of SOCM, ΣSOCM, C_0 and k to habitat modification, following Hedges et al. (1999), Luo et al. (2006) and Tan et al. (2019). A total of 21 sites with data for treatment groups (habitats after modification) and control groups (habitats before modification) were used to calculate the natural logarithm of RR (lnRR):

$$\ln\mathrm{RR} = \ln\left(\frac{\overline{\mathrm{X}}_{\mathrm{T}}}{\overline{\mathrm{X}}_{\mathrm{C}}}\right) = \ln\left(\overline{\mathrm{X}}_{\mathrm{T}}\right) - \ln\left(\overline{\mathrm{X}}_{\mathrm{C}}\right) \qquad \text{Eq.(7)}$$

where the subscripts T and C denote treatment and control groups, respectively; X denotes the mean value of the parameter (SOCM, ΣSOCM, C_0 or k). The variance (v) was calculated as:

$$v = \frac{S_{\mathrm{T}}^2}{n_{\mathrm{T}}\overline{\mathrm{X}}_{\mathrm{T}}^2} + \frac{S_{\mathrm{C}}^2}{n_{\mathrm{C}}\overline{\mathrm{X}}_{\mathrm{C}}^2} \qquad \text{Eq.(8)}$$

where n denotes the sample size and S the standard deviation.

We also calculated a weighted response ratio (RR_{++}) from individual RR_{ij} (i = 1, 2, 3,...., m; j = 1, 2, 3,...., y_i) pairwise comparison between treatment and control groups:

$$\mathrm{RR}_{++} = \frac{\sum_{i=1}^{m}\sum_{j=1}^{y_i} w_{ij}\mathrm{RR}_{ij}}{\sum_{i=1}^{m}\sum_{j=1}^{y_i} w_{ij}} \qquad \text{Eq.(9)}$$

where m is the number of groups (different habitat types), y_i is the number of comparisons in the ith group, and w_{ij} is the weighting factor. w_{ij} and the standard error ($\mathrm{s}(\mathrm{RR}_{++})$) were calculated as follows:

$$w_{ij} = \frac{1}{v} \qquad \text{Eq.(10)}$$

$$s(\mathrm{RR}_{++}) = \sqrt{\frac{1}{\sum_{i=1}^{m}\sum_{j=1}^{y_i} w_{ij}}} \qquad \text{Eq.(11)}$$

The 95% confidence interval (95% CI) for the log response ratio was estimated as:

$$95\%\ \mathrm{CI} = \mathrm{RR}_{++} \pm 1.96\ s(\mathrm{RR}_{++}) \qquad \text{Eq.(12)}$$

If the 95% CI did not overlap with zero, the response of the concerned variable to habitat modification was considered significant.

2.7. Statistical Analysis.

All data were tested for normality and homogeneity of variance. Significant differences in environmental factors, SOCM, ΣSOCM and SOC mineralization parameters [ΔC_0, Δk, and $\Delta(C_0/\mathrm{SOC})$] among habitat types were tested by analysis of variance (ANOVA) followed by pairwise comparisons. Pearson correlation analysis was used to examine the relationships between ΣSOCM (or SOC mineralization parameters) and environmental variables. Redundancy analysis (RDA) was performed to determine which ΔEF best explained the variability in ΔSOCCM [or ΔC_0, Δk and $\Delta(C_0/SOC)$]; input parameters for the analysis include ΔpH, Δsalinity, ΔSWC, ΔBD, ΔNH_4^+–N, ΔNO_3^-–N, ΔCl^-, ΔSO_4^{2-}, ΔC:N, ΔSOC, ΔMBC, ΔMBN and ΔSPS. ANOVA and Pearson correlation analysis were done in SPSS 17.0 (SPSS Inc., USA); RDA was done in CANOCO 5.0 for Windows (Microcomputer Power, Ithaca, USA). All results were considered significant at $p < 0.05$ and were summarized as mean ± 1 standard error, unless otherwise stated. Sampling site map, statistical plots and conceptual diagrams were produced using ArcGIS 10.2 (ESRI Inc., Redlands, CA, USA), OriginPro 9.0 (OriginLab Corp. USA) and EDraw Max version 7.3 (EdrawSoft, Hong Kong, China), respectively.

3. Results

3.1. Soil Properties Across Habitat Types.

The soil physicochemical properties were shown in Figure 2. There were no significant differences in mean soil pH (Figure 2a), salinity (Figure 2b), bulk density (Figure 2d), Cl^- (Figure 2e), MBC (Figure 2h), soil C:N (Figure 2i) or soil particle size (Figs 2j-l) among the three habitat types ($p > 0.05$), but there were significant differences for the other parameters. Soil SO_4^{2-} (Figure 2f) were higher in aquaculture ponds (APs) than in mud flats (MFs) and *S. alterniflora* marshes (SAs) ($p < 0.05$ or < 0.01). Soil water content was higher in SAs and APs than in MFs ($p < 0.05$; Figure 2c). SOC (Figure 2g) was higher in SAs, followed by APs and MFs ($p < 0.01$).

3.2. Soil Organic Carbon Mineralization (SOCM) Rate

Across all sampling sites, the rate of CO_2 production from anaerobic SOC mineralization averaged 11.9 ± 1.6 μg g^{-1} d^{-1} in MFs, 20.4 ± 2.1 μg g^{-1} d^{-1} in SAs, and 16.9 ± 2.3 μg g^{-1} d^{-1} in APs (Figure 3a). Overall, CO_2 production rate decreased significantly among the three habitats in the order of SAs > APs > MFs ($p<0.01$). The rate of CH_4 production from SOC mineralization averaged 5.0 ± 1.4 ng g^{-1} d^{-1} in the MFs, 25.8 ± 2.8 ng g^{-1} d^{-1} in SAs, and 14.3 ± 1.3 ng g^{-1} d^{-1} in the APs (Figure 3b). Like CO_2, CH_4 production rate decreased significantly among the three habitats in the order of SAs > APs > MFs ($p<0.01$).

The SOCM rates for the different wetland habitat types are shown in Figure 4 and Figure S1. Because CO_2 production rates were 1000-fold higher than CH_4 production rates on a per mass basis, the SOCM rates were mainly driven by mineralization of SOC into CO_2. Across all sampling sites, the mean SOCM rates varied in the range of 3.9–20.5 μg g^{-1} d^{-1} for MFs, 7.2–38.2 μg g^{-1} d^{-1} for SAs, and 6.6–30.0 μg g^{-1} d^{-1} for APs (Figure 4a). The measured rates peaked on the 3rd day in all habitat types, then steadily decreased toward the end of the incubation (Figure 4a). The SOCM rate was significantly higher in SAs (20.4 ± 2.1 μg g^{-1} d^{-1}), followed by APs (16.9 ± 2.4 μg g^{-1} d^{-1}) and MFs (11.9 ± 1.7 μg g^{-1} d^{-1}) (p<0.05 or <0.01) (Figure 4b).

3.3. Cumulative Soil Organic Carbon Mineralization (ΣSOCM)

ΣSOCM during the 60-d incubation period for the different wetland habitat types is shown in Figure 5 and Figure S2. ΣSOCM across all sampling sites was 35.5–186.9 μg g^{-1} in MFs, 59.2–284.0 μg g^{-1} in SAs, and 49.8–271.4 μg g^{-1} in APs (Figure S2). ΣSOCM increased initially but then approached a plateau toward the end of the incubation, and the values increasingly diverged from one another among the three habitat types (Figure 5a) and there were significant differences among the three habitats (p<0.05 or <0.01) (Figure 5b). The mean ΣSOCM was highest in SAs (111.5 ± 12.6 μg g^{-1}), followed by APs (90.0 ± 12.8 μg g^{-1}) and MFs (65.2 ± 9.0 μg g^{-1}). At the end of the 60-day incubation, the mean $\Sigma SOCM_{final}$ was 95.0, 163.0 and 135.0 μg g^{-1} for MFs, SAs and APs, respectively (Table 1).

3.4. First-Order Kinetic Model for Carbon Mineralization.

To better compare the mineralization processes across the wetland habitat types, the data were fitted to a first-order kinetic model. The values of the fitting parameters C_0 (initial bioavailable SOC) and k (mineralization rate constant) are listed in Table 1 and Table S1. Across all the sampling sites, C_0 varied in the range of 48.1–252.3 μg g^{-1} for MFs, 80.2–373.2 μg g^{-1} for SAs, and 67.8–365.7 μg g^{-1} for APs (Table S1). The mean C_0 was highest in SAs (152.3 μg g^{-1}), followed by APs (125.6 μg g^{-1}) and MFs (88.8 μg g^{-1}) (Table 1). MFs had a higher mean k but lower C_0/SOC than the other two habitats (Table 1). The $\Sigma SOCM_{final}/C_0$ values varied by less than 0.5% among the three habitats (Table 1). The goodness of fit values (Adj. R^2) of the equations were all better than 0.94 (Table 1).

3.5. Response of Carbon Mineralization Parameters to Habitat Modification.

The Weighted response ratios (RR_{++}) of SOCM, ΣSOCM, C_0 and k are shown in Figure 6. Conversion of MFs to SAs significantly (p<0.05) increased SOCM by 43.4% (range 21.9–61.1 %; Figure 6a), ΣSOCM by 40.4% (range 21.9–48.4 %; Figure 6b) and C_0 by 47.9% (Figure 6c). However, conversion of SAs to APs significantly (p<0.05) decreased SOCM by 22.2% (range 8.9–30.4 %; Figure 6a), ΣSOCM by 21.8% (range 16.0–31.5 %; Figure 6b), and C_0 by 24.5% (Figure 6c). Moreover, MF-to-SA and SA-to-AP conversions significantly increased k by 3.2% and 2.9%, respectively (p<0.05) (Figure 6d).

3.6. Change in Soil Organic Carbon Mineralization and its Environmental Drivers.

Based on redundancy analysis (RDA), changes in EF (ΔEF) presented in the ordination explained 69.0% of the variability in ΔΣSOCM, ΔC_0, Δk, and $\Delta(C_0/SOC)$ in the case of MF-to-SA conversion (Figure 7a), and 64.1% in the case of SA-to-AP conversion (Figure

7b). Overall, ΔSOC was the most important driver of ΔΣSOCM in both scenarios of habitat modification, explaining 45.5% of the variability when MFs were converted to SAs (Figure 7a), and 37.2% when SAs were converted to APs (Figure 7b). Interestingly, ΔNH_4^+-N was only a minor factor (4.8%) in MFs-to-SAs conversion, but it became the second main driver (16.2%) in SAs-to-APs conversion; ΔSO_4^{2-} played a slightly larger role in the latter scenario (6.4% vs. 8.5%). The correlation coefficients between changes in ΣSOCM, C_0, k and C_0/SOC and the different environmental variables for the different cases of habitat modification are shown in Table 2.

4. Discussion

4.1. Comparison of Soil Properties Among Habitat Types

Previous studies have shown that the soil physicochemical properties are sensitive to environmental changes and anthropogenic disturbances (e.g., Gao et al., 2019; Mueller et al., 2016; Wang et al., 2019). In the present study, we assessed the response of soil properties to habitat modification in impacted coastal wetlands in China. Among the variables examined, only soil SOC and SO_4^{2-} differed significantly among the three habitat types. The soil SO_4^{2-} in APs was about twice the concentration in MFs and SAs (Figure 2f). Similar results were reported earlier that soil SO_4^{2-} in the aquaculture ponds was 3–5 times higher than the natural saltmarsh (Gao et al., 2019). While SO_4^{2-} in the soil could be converted to H_2S by sulfate reducing bacteria under anaerobic condition and be lost from the system, the much larger volume of saltwater in APs might be able to replenish SO_4^{2-} more quickly, thereby maintaining a higher SO_4^{2-} concentration in the soil.

Additional SO_4^{2-} may have also originated from aquaculture feeds and pond disinfectants (Feng, 2014; Zou et al., 2022).

Contrary to the expectation that use of feeds would increase the soil carbon content in aquaculture ponds, we found SOC in APs was significantly lower than SAs (Figure 2g). The results could be primarily attributed to higher productivity of the marsh vegetation leading to larger inputs of plant litter and root exudates into the soil (Mueller et al., 2016; Xia et al., 2021), which were eliminated when the vegetation was removed to create the aquaculture ponds. By comparison, SOC in the mudflats was the lowest likely due to the lack of autochthonous or allochthonous carbon inputs.

4.2. Production of Carbon Greenhouse Gases Among Habitat Types

Organic carbon in waterlogged soil is mineralized primarily via anaerobic microbial metabolism (e.g., Hopfensperger et al., 2014; Kostka et al., 2002), with CO_2 as the main by-product (e.g., Gribsholt & Kristensen, 2003; Kim et al., 2015; Luo et al., 2019b). This is consistent with our observations that CO_2 production rates were 1000-fold higher than CH_4 production rates on a per mass basis (Figure 3). Similar to earlier observations (Boulogne et al., 2016; Keller et al., 2015; Kim et al., 2015), it appeared that the bacterial communities required about three days to acclimate to the experimental condition before they reached maximum SOC mineralization rates, after which the rates decreased as labile organic carbon became depleted (Figure 4a).

It is worth noting that CO_2 and CH_4 production in our study was measured by incubation of slurries, which may not reflect the dynamic condition *in situ* where river flow and periodic tidal flushing would change the soil conditions (Wells et al., 2018) and affect CO_2 and CH_4 production. Therefore, future research may consider *in situ* measurements using tracer technique, without the need for incubation, to give more accurate gas production rates.

4.3. Responses of Soil Carbon Turnover to Habitat Modification

The differences in SOC mineralization rate and cumulative SOC mineralization among the three habitat types (Figs. 4b and 5b) followed the differences in their SOC content (Figure 2g), showing that *S. alterniflora* invasion and aquaculture operation both increased labile soil organic substrates and subsequent mineralization activities relative to the native mudflats. Nevertheless, based on the first-order kinetic model, C_0/SOC was all under 0.02 (Table 1), meaning that < 2% of the soil organic carbon was bioavailable to microbes (labile to semi-labile), and the vast majority might be considered as refractory for longer-term burial. Our data also suggest that all bioavailable carbon was mineralized within 60 days, and the value of $\Sigma SOCM_{final}/C_0$ being slightly higher than 1 may be indicative of inherent uncertainty in deriving C_0 from curve fitting, or labile C_0 facilitating mineralization of some of the refractory carbon (i.e., priming effect; Guenet et al., 2010). Based on our incubation experiments, the CO_2 production rate averaged 1.6 g C kg^{-1} yr^{-1} across the coastal wetlands in our study. Assuming this represented the labile fraction of carbon deposition, the corresponding potential burial of refractory carbon would be ~8.4 g C kg^{-1} yr^{-1}. Given the measured soil bulk density of 1300 kg m^{-3} and a median sediment accretion rate of ~3.4 cm yr^{-1} in coastal marshes in China (Wang et al., 2006), the estimated carbon burial rate would be ~370 g C m^{-2} yr^{-1}. This is comparable to the estimated mean carbon accumulation rate (~200 g C m^{-2} yr^{-1}) for tidal wetlands in China in a recent study (Wang et al., 2021; their Fig. 2).

Because habitat types affect both carbon deposition (as indicated by SOC and C_0 data) and carbon mineralization (ΣSOCM), we may derive a 'Habitat Ratio' using data from Figure 2 and Table 1 to compare their overall carbon source-sink dynamics (Table 3). Comparison of the Habitat Ratio between SAs and APs showed that the former had higher organic carbon deposition, bioavailable carbon and cumulative C mineralization, but all by a similar extent (20–21%); therefore, the soil carbon source-sink dynamics did not appear to be different between the two habitat types. On the other hand, SAs had 50% higher SOC than MFs but 71–72% higher bioavailable carbon and carbon mineralization, suggesting that SAs functioned as more concentrated stocks of labile soil organic carbon and stronger net carbon emission sources relative to MFs. This is consistent with others' observations showing an increase in labile organic carbon fraction in *S. alterniflora* soil with time (Cui et al., 2021), but it contradicts another study suggesting that *S. alterniflora* invasion of mudflat decreased the labile organic carbon pool in the soil (Yang et al., 2013). The differences could be due to the fact that Yang et al. (2013) measured carbon mineralization under aerobic condition, which did not represent the water-logged, low-oxygen condition of the soil and which would have suppressed methanogenesis and underestimated the labile carbon turn-over. APs had 25% higher SOC, but 41–42% higher bioavailable carbon and carbon mineralization than MFs, reflecting the high amounts of sedimented labile organics from excess feeds and biological productivity in the ponds (Yang et al., 2022).

4.4. Implications for Coastal Biogeochemistry

Continuous land development and land use change has drastically altered the coastal landscape of China (Cui et al., 2016; Meng et al., 2017). Based on our findings, conversion of mudflats to *Spartina* marshes increased soil organic carbon mineralization, but conversion of *Spartina* marshes to aquaculture ponds decreased soil organic carbon mineralization (Figure 8)—This was consistent across all sites over a large latitudinal range, independent of differences in local geography, land management practices or climate conditions. In both land change scenarios, soil organic carbon was the overwhelming factor (37.2–45.5 %) that determined the mineralization activity.

The invasive *S. alterniflora* was introduced to China originally to protect mudflats against erosion, and it has proliferated along the coast since (An et al., 2007). Meanwhile, increasing food demand has led to rapid expansion of coastal aquaculture in China (Ren et al., 2019). While on-the-ground census data are rare, scientists used remote sensing methods to estimate the historical change in areal coverage by *S. alterniflora* marshes (Mao et al., 2019) and coastal aquaculture ponds (Duan et al., 2021) in the recent decades. Combining these literature data with our measured habitat-specific soil CO_2 and CH_4 production potentials, we calculated the total CO_2-eq production in the 20 cm topsoil, considering CH_4 has 45 times the 100-year warming potential as CO_2 (Neubauer & Megonigal, 2015); we further assessed landscape change effect by estimating the net increase in soil CO_2-eq production relative to native mudflats. Our calculations suggest that total soil CO_2-eq production increased 12-fold as *S. alterniflora* marshes spread along China's coast, whereas the expanding aquaculture activities increased total soil CO_2-eq production ~1.6 fold during the past three decades (Figure 9). The estimated land coverage by coastal aquaculture ponds was an order of magnitude larger than *S. alterniflora* marshes; consequently, the net increase in soil CO_2-eq production relative to native mudflats was largely driven by the large-scale conversion of coastal land to aquaculture ponds (Figure 9). Nevertheless, the total area of coastal aquaculture ponds appeared to have plateaued in recent years and therefore the contribution of soil CO_2-eq production from coastal aquaculture is expected to remain stable at ~4.3 Tg yr^{-1}. Meanwhile, if *S. alterniflora* marsh expansion continues along the trajectory, it is expected to cause further net increase in soil CO_2-eq production to ~0.7 Tg yr^{-1} by end of this decade.

5. Conclusions and recommendations

The coastal mudflat habitats of China have undergone drastic changes in the recent decades due to the spread of the invasive *S. alterniflora* and conversion to aquaculture ponds. We showed that these land use change increased the total and labile fractions of soil organic carbon, carbon mineralization rate as well as greenhouse gas production relative to the native mudflats, and the effects were consistent across a wide latitudinal range and climate gradient (Figure 8). As the areal coverage of *S. alterniflora* marshes and coastal aquaculture ponds continue to increase, we may expect a net increase in carbon greenhouse gas production and emission along the coast. This study provides a better insight into assessing the effects of land use and land cover change (LULCC) on coastal wetland carbon biogeochemical cycle process and land surface greenhouse gas emission across a large geographical range.

Several recommendations should be considered in future study: 1) Accurate census and monitoring of coastal habitats including small-hold aquaculture ponds is much needed in China and it will improve our assessment of landscape change effects on coastal carbon and greenhouse gas dynamics. 2) While we measured greenhouse gas production in soils, the actual emissions to the atmosphere could be further modulated by in situ physical (e.g., water turbulence, wind) and biological factors (e.g., consumption by microbes). Measurements of in situ emissions from the different habitats, using methods such as flux chambers, will be valuable. 3) Lastly, most of our sampling sites were concentrated in the northeastern part of the coast. Additional sampling in the southern provinces would allow data analysis based on a finer spatial resolution.

Conflict of Interest

The authors declare no conflicts of interest relevant to this study

Data Availability Statement

The data used in this study are available in the Mendeley research data repository: Yang et al. (2022), Ancillary variables, SOC mineralization parameters, and carbon greenhouse gases production potential in impacted coastal wetlands across a wide latitudinal range in China, Mendeley Data, V1 (https://doi.org/10.17632/3r2827w6f4.1).

Acknowledgements

This research was supported by the National Science Foundation of China (No. 41801070, 41671088), the National Science Foundation of Fujian Province (No. 2020J01136, 2019J05067), the Minjiang Scholar Programme. We would like to thank Yifei Zhang, Chen Tang, Guanghui Zhao and Ling Li of the School of Geographical Sciences, Fujian Normal University, for their field assistance. We thank the Associate Editor and Reviewers for their comments and suggestions that have helped improve the manuscript.

References

An, S. Q., Gu,B.H., Zhou, C. F., Wang, Z. S., & Liu, Y. H . (2007). *Spartina* invasion in China: implications for invasive species management and future research. *Weed Research, 47*(3), 183–191. https://doi.org/10.1111/j.1365-3180.2007.00559.x

Andreetta, A., Huertas, A. D., Lotti, M., & Cerise, S. (2016). Land use changes affecting soil organic carbon storage along a mangrove swamp rice chronosequence in the Cacheu and Oio regions (northern Guinea-Bissau). *Agriculture Ecosystems & Environment*, *216*, 314–321. https://doi.org/10.1016/j.agee.2015.10.017

Boulogne, I., Ozier-Lafontaine, H., Merciris, P., Vaillant, J., Labonte, L., & LorangerMerciris, G. (2016). Soil chemical and biological characteristics influence mineralization processes in different stands of a tropical wetland. *Soil Use and Management*, *32*(3), 269–278. https://doi.org/10.1111/sum.12273

Chen, B. B., & Sun, Z. G. (2020). Effects of nitrogen enrichment on variations of sulfur in plant-soil system of *Suaeda salsa* in coastal marsh of the Yellow River estuary. China. *Ecological Indicators*, 109, 105797. https://doi.org/10.1016/j.ecolind.2019.105797

Cooper, J. M., Burton, D., Daniell, T. J., Griffiths, B. S., Zebarth, B. J. (2011). Carbon mineralization kinetics and soil biological characteristics as influenced by manure addition in soil incubated at a range of temperature. *European Journal of Soil Biology*, *47*(6), 392–399. https://doi.org/10.1016/j.ejsobi.2011.07.010

Cui, B. S., He, Q., Gu, B. H., Bai, J. H., & Liu, X. H. (2016). China's coastal wetlands: understanding environmental changes and human impacts for management and conservation. *Wetlands*, *36*(S1), S1–S9. https://doi.org/10.1007/s13157-016-0737-8

Cui, L. N., Sun, H. M., Du, X. H., Feng, W. T., Wang, Y. G., Zhang, J. C., et al. (2021). Dynamics of labile soil organic carbon during the development of mangrove and salt marsh ecosystems. *Ecological Indicators*, *129*, 107875. http://dx.doi.org/10.1016/j.ecolind.2021.107875

Davidson, N. C. (2014). How much wetland has the world lost? Long-term and recent trends in global wetland area. *Marine and Freshwater Research*, *65*, 934–941. http://dx.doi.org/10.1071/MF14173

Dick, T. M., & Osunkoya, O. O. (2000). Influence of tidal restriction floodgates on decomposition of mangrove litter. *Aquatic Botany*, *68*, 273–280. https://doi.org/10.1016/S0304-3770(00)00119-4

Drake, K., Halifax, H., Adamowicz, S. C., & Craft, C. (2015). Carbon sequestration in tidal salt marshes of the Northeast United States. *Environmental Management*, *56*, 998–1008. https://doi.org/10.1007/s00267-015-0568-z

Duan, Y. Q., Li, X., Zhang, L. P., Chen, D., Liu, S. A., & Ji, H. Y. (2020). Mapping national-scale aquaculture ponds based on the Google Earth Engine in the Chinese coastal zone. *Aquaculture*, *520*, 734666. https://doi.org/10.1016/j.aquaculture.2019.734666

Duan, Y. Q., Tian, B., Li, X., Liu, D. Y., Sengupta, D., Wang, Y. J., et al. (2021). Tracking changes in aquaculture ponds on the China coast using 30 years of Landsat images. *International Journal of Applied Earth Observation and Geoinformation*, *102*, 102383. https://doi.org/10.1016/j.jag.2021.102383

Feng, Q. F. (2014). The sulfide content in sediment of freshwater shrimp ponds and relationship between sulfide and other parameters. Shanghai: Shanghai Ocean University. (in Chinese, master's thesis)

Gao, D. Z., Chen, G. X., Li, X. F., Lin, X. B., & Zeng, C. S. (2018a). Reclamation culture alters sediment phosphorus speciation and ecological risk in coastal zone of Southeastern China. *Clean-Soil, Air, Water*, *46*(11), 1700495.

https://doi.org/10.1002/clen.201700495

Gao, D. Z., Liu, M., Hou, L. J., Derrick, Y. F. L., Wang, W. Q., Li, X. F., et al. (2019). Effects of shrimp-aquaculture reclamation on sediment nitrate dissimilatory reduction processes in a coastal wetland of southeastern China. *Environmental Pollution*, *255*, 113219. https://doi.org/10.1016/j.envpol.2019.113219

Gao, G. F., Li, P. F., Shen, Z. J., Qin, Y. Y., Zhang, X. M., Ghoto, K., Z., et al. (2018b). Exotic *Spartina alterniflora* invasion increases CH_4 while reduces CO_2 emissions from mangrove wetland soils in southeastern China. *Scientific Reports*, *8*, 9243. https://doi.org/10.1038/s41598-018-27625-5

Gao, J. H., Feng, Z. X., Chen, L., Wang, Y. P., Bai, F. L., & Li, J. (2016). The effect of biomass variations of *Spartina alterniflora* on the organic carbon content and composition of a salt marsh in northern Jiangsu Province, China. *Ecological Engineering*, *95*, 160–170. http://dx.doi.org/10.1016/j.ecoleng.2016.06.088

Gribsholt, B., & Kristensen, E. (2003). Benthic metabolism and sulfur cycling along an inundation gradient in a tidal *Spartina anglica* salt marsh. *Limnology and Oceanography*, *48*(6), 2151–2162. https://doi.org/10.4319/lo.2003.48.6.2151

Guenet, B., Danger, M., Abbadie, L., & Lacroix, G. (2010). Priming effect: bridging the gap between terrestrial and aquatic ecology. *Ecology*, *91*(10), 2850-2861. https://doi.org/10.1890/09-1968.1

Hedges, L. V., Gurevitch, J., & Curtis, P. S. (1999). The meta-analysis of response ratios in experimental ecology. *Ecology*, *80*, 1150–1156. https://doi.org/10.2307/177062

Hopfensperger, K. N., Burgin, A. J., Schoepfer, V. A., & Helton, A. M. (2014). Impacts of saltwater incursion on plant communities, anaerobic microbial metabolism, and resulting relationships in a restored freshwater wetland. *Ecosystems*, *17*(5), 792–807. https://doi.org/10.1007/s10021-014-9760-x

Hyvonen, R., Agren G. I., & Dalias, P. (2005). Analysing temperature response of decomposition of organic matter. *Global Change Biology*, *11*(5), 770–778. https://doi.org/10.1111/j.1365-2486.2005.00947

Hyun, J. -H., Smith, A. C., & Kostka, J. E. (2007). Relative contributions of sulfate-and iron (III) reduction to organic matter mineralization and process controls in contrasting habitats of the Georgia saltmarsh. *Applied Geochemistry*, *22*(12), 2637–2651. https://doi.org/10.1016/j.apgeochem.2007.06.005

Kane, E. S., Chivers, M. R., Turetsky, M. R., Treat, C. C., Petersen, D. G., Waldrop, M., et al. (2013). Response of anaerobic carbon cycling to water table manipulation in an Alaskan rich fen. *Soil Biology & Biochemistry*, *58*(2), 50–60. https://doi.org/10.1016/j.soilbio.2012.10.032

Kayranli, B., Scholz, M., Mustafa, A., & Hedmark, Å. (2010). Carbon storage and fluxes within freshwater wetlands: A critical review. *Wetlands*, *30*, 111–124. https://doi.org/10.1007/s13157-009-0003-4

Keller, J. K., White, J. R., Bridgham, S. D., & Pastor, J. (2004). Climate change effects on carbon and nitrogen mineralization in peatlands through changes in soil quality. *Global Change Biology*, *10*, 1053–1064. http://dx.doi.org/10.1111/j.1529-8817.2003.00785.x

Kim, Y., Ullah, S., Roulet, N. T., & Moore, T. R. (2015). Effect of inundation, oxygen and temperature on carbon mineralization in boreal ecosystems. *Science of the Total Environment*, *511*, 381–392. http://dx.doi.org/10.1016/j.scitotenv.2014.12.065

Kostka, J. E., Roychoudhury, A., & Van Cappellen, P. (2002). Rates and controls of anaerobic microbial respiration across spatial and temporal gradients in saltmarsh sediments. *Biogeochemistry*, *60*(1), 49–76. https://doi.org/10.1023/A:1016525216426

Kirwan, M. L., & Megonigal, J. P. (2013). Tidal wetland stability in the face of human impacts and sea-level rise. *Nature*, 504, 53–60. https://doi.org/10.1038/nature12856

Li, X. F., Han, S. J., Guo, Z. L., Shao, D. K., & Xin, L. H. (2010). Changes in soil microbial biomass carbon and enzyme activities under elevated CO_2 affect fine root decomposition processes in a Mongolian oak ecosystem. *Soil Biology & Biochemistry*, *42*, 1101–1107. https://doi.org/10.1016/j.soilbio.2010.03.007

Liu, M. Y., Mao, D. H., Wang, Z. M., Li, L., Man, W. D., Jia, M. M., et al. (2018). Rapid invasion of *Spartina alterniflora* in the coastal zone of mainland China: new observations from landsat OLI images. *Remote Sensing*, *10*, 1933. https://doi.org/10.3390/rs10121933

Liu, J. E., Han, R. M., Su, H. R., Wu, Y. P., Zhang, L. M., Richardson, C. J., et al. (2017). Effects of exotic *Spartina alterniflora* on vertical soil organic carbon distribution and storage amount in coastal salt marshes in Jiangsu, China. *Ecological Engineering*, *106*, 132–139. http://dx.doi.org/10.1016/j.ecoleng.2017.05.041

Luo, M., Zhu, W.F., Huang, J.F., Liu, Y. X., Duan, X., Wu, J., et al. (2019a). Anaerobic organic carbon mineralization in tidal wetlands along a low-level salinity gradient of a subtropical estuary: Rates, pathways, and controls. *Geoderma*, *337*, 1245–1257. https://doi.org/10.1016/j.geoderma.2018.07.030

Luo, M., Huang, J. F., Zhu, W. F., & Tong, C. (2019b). Impacts of increasing salinity and inundation on rates and pathways of organic carbon mineralization in tidal wetlands: a review. *Hydrobiologia*, 827, 31–49. https://doi.org/10.1007/s10750-017-3416-8

Luo, Y. Q., Hui, D. F., & Zhang, D. Q. (2006). Elevated CO_2 stimulates net accumulations of carbon and nitrogen in land ecosystems: A meta-analysis. *Ecology*, *87*, 53–63. https://doi.org/10.1890/04-1724

Mao, D. H., Liu, M. Y., Wang, Z. M., Li, L., Man, W. D., Jia, M. M., et al. (2019). Rapid invasion of *Spartina alterniflora* in the coastal zone of mainland China: spatiotemporal patterns and human prevention. *Sensors*, 19, 2308. https://doi.org/10.3390/s19102308

Meng, W. Q., He, M. X., Hu, B. B., Mo, X. Q., Li, H. Y., Liu, B. Q., et al. (2017). Status of wetlands in China: A review of extent, degradation, issues and recommendations for improvement. *Ocean & Coastal Management*, *146*, 50–59. http://dx.doi.org/10.1016/j.ocecoaman.2017.06.003

Mitsch, W. J., Bernal, B., Nahlik, A. M., Mander, Ü., Zhang, L., Anderson, C. J., et al. (2013). Wetlands, carbon, and climate change. *Landscape Ecology*, *28*(4), 583–597. https://doi.org/10.1007/s10980-012-9758-8

Mueller, P., Jensen, K., & Megonigal, J. P. (2016). Plants mediate soil organic matter decomposition in response to sea level rise. *Global Change Biology*, *22*(1), 404–414. https://doi.org/10.1111/gcb.13082

Neubauer, S. C., & Megonigal, J. P. (2015). Moving beyond global warming potentials to quantify the climatic role of ecosystems. *Ecosystems*, 18(6),

https://doi.org/1000–1013. doi:10.1007/s10021-015-9879-4
Su, J., Friess, D. A., Gasparatos, A. (2021). A meta-analysis of the ecological and economic outcomes of mangrove restoration. *Nature Communications*, 12, 5050. https://doi.org/10.1038/s41467-021-25349-1
Sun, Z. G., Sun, W. G., Tong, C., Zeng, C. S., Yu, X., & Mou, X. J. (2015). China's coastal wetlands: Conservation history, implementation efforts, existing issues and strategies for future improvement. *Environment International*, *79*, 25–41. http://dx.doi.org/10.1016/j.envint.2015.02.017
Packalen, M. S., Finkelstein, S. A., McLaughlin, J. W. (2014). Carbon storage and potential methane production in the Hudson Bay Lowlands since mid-Holocene peat initiation. *Nature Communications*, 5, 4078. https://doi.org/10.1038/ncomms5078
Percival, J., & Lindsay, P. (1997). Measurement of physical properties of sediments. In: Mudrock, A., Azcue, J. M., & Mudrock, P. (Eds.), Manual of Physico-Chemical Analysis of Aquatic Sediments. CRC Press, New York, USA, pp. 7–38.
Piper, C. L., Siciliano, S. D., Winsley, T., & Lamb, E. G. (2015). Smooth brome invasion increases rare soil bacterial species prevalence, bacterial species richness and evenness. *Journal of Ecology*, *103*, 386–396. https://doi.org/10.1111/1365-2745.12356
Tan, L. S., Ge, Z. M., Zhou, X. H., Li, S. H., Li, X. Z., & Tang, J. W. (2020). Conversion of coastal wetlands, riparian wetlands, and peatlands increases greenhouse gas emissions: A global meta-analysis. *Global Change Biology*, *26*, 1638–1653. http://dx.doi.org/10.1111/gcb.14933
Templer, P., Findlay, S., & Lovett, G. (2003). Soil microbial biomass and nitrogen transformations among five tree species of the Catskill Mountains, New York, USA. *Soil Biology & Biochemistry*, *35*(4), 607–613. http://dx.doi.org/10.1016/s0038-0717(03)00006-3
Tong, C., Wang, W. Q., Zeng, C. S., & Marrs, R. (2010). Methane (CH_4) emission from a tidal marsh in the Min River estuary, Southeast China. *Journal of Environmental Science and Health, Part A*, *45*(4), 506–516. https://doi.org/10.1080/10934520903542261

Ren, C. Y., Wang, Z. M., Zhang, Y. Z., Zhang, B., Chen, L., Xia, Y. B., et al. (2019). Rapid expansion of coastal aquaculture ponds in China from Landsat observations during 1984–2016. *International Journal of Applied Earth Observation and Geoinformation*, *82*, 101902. https://doi.org/10.1016/j.jag.2019.101902

Vance, E.D., Brookes, P.C., & Jenkinson, D. S. (1987). An extraction method for measuring soil microbial biomass C. *Soil Biology & Biochemistry*, *19*, 703–707. https://doi.org/10.1016/0038-0717(87)90052-6

Vizza, C., West, W. E., Jones, S. E., Hart, J. A., & Lamberti, G. A. (2017). Regulators of coastal wetland methane production and responses to simulated global change. *Biogeosciences, 14*, 431–446. https://doi.org/10.5194/bg-14-431-2017

Walker, L. R., & Smith, S. D. (1997). Impacts of invasive plants on community and ecosystem properties. In: Luken, J.O., & Thieret, J. W. (eds) Assessment and management of plant invasion. Spriger-Verlag, New York, pp 69–94.

Wang, A. J., Gao, S., & Jia J. J. (2006). Impact of the cord-grass *Spartina alterniflora* on sedimentary and morphological evolution of tidal salt marshes on the Jiangsu coast, China. *Acta Oceanologica Sinica*, 25, 32–42.

Wang, F. M., Sanders, C. J., Santos, I. R., Tang, J. W., Schuerch, M., Kirwan, M. L., et al. (2021). Global blue carbon accumulation in tidal wetlands increases with climate change. *National Science Review*, 8, nwaa296. https://doi.org/10.1093/nsr/nwaa296

Wang, M. E., Markert, B., Shen, W. M., Chen, W. P., Peng, C., & Ouyang, Z. Y. (2011). Microbial biomass carbon and enzyme activities of urban soils in Beijing. *Environmental Science and Pollution Research*, *18*, 958–967. https://doi.org/10.1007/s11356-011-0445-0

Wang, W. Q., Sardans, J., Wang, C., Zeng, C. S., Tong, C., Chen, G. X., et al. (2019). The response of stocks of C, N, and P to plant invasion in the coastal wetlands of China. *Global Change Biology*, *25*(2), 733–743. https://doi.org/10.1111/gcb.14491

Wassmann, R., Neue, H. U., Bueno, C., Lantin, R. S., Alberto, M. C. R., Buendia, L. V., et al. (1998). Methane production capacities of different rice soils derived from inherent and exogenous substrates. *Plant and Soil*, *203*, 227–237. https://doi.org/10.1023/A:1004357411814

Wells, N. S., Maher, D. T., Erler, D. V., Hipsey, M., Rosentreter, J. A., & Eyre, B. D. (2018). Estuaries as sources and sinks of N_2O across a land use gradient in subtropical Australia. *Global Biogeochemical Cycles*, *32*(5), 877–894. https://doi.org/10.1029/2017gb005826

Wen, Y. L., Bernhardt, E. S., Deng, W. B., Liu, W. J., Yan, J. X., Baruch, E. M., et al. (2019). Salt effects on carbon mineralization in southeastern coastal wetland soils of the United States. *Geoderma,* *339*, 31–39. https://doi.org/10.1016/j.geoderma.2018.12.035

Xia, S. P., Wang, W. Q., Song, Z. L., Kuzyakov, Y., Guo, L. D., Van Zwieten, L., et al. (2021). *Spartina alterniflora* invasion controls organic carbon stocks in coastal marsh and mangrove soils across tropics and subtropics. *Global Change Biology*, *27*(8), 1627–1644. https://doi.org/110.1111/gcb.15516

Yang, P., Bastviken, D., Jin, B. S., Mou, X. J., & Tong, C. (2017). Effects of coastal marsh conversion to shrimp aquaculture ponds on CH_4 and N_2O emissions. *Estuarine, Coastal and Shelf Science*, 199, 125–131. https://doi.org/10.1016/j.ecss.2017.09.023

Yang, P., Lu, M. H., Tang, K. W., Yang, H., Lai, D. Y. F., Tong, C., et al. (2021). Coastal reservoirs as a source of nitrous oxide: Spatio-temporal patterns and assessment strategy. *Science of the Total Environment*, *790*, 147878. https://doi.org/10.1016/j.scitotenv.2021.147878

Yang, P., Tang, K. W., Yang, H., Tong, C., Yang, N., Lai, D. Y. F., et al. (2022). Insights into the farming-season carbon budget of coastal earthen aquaculture ponds in southeastern China. *Agriculture, Ecosystems and Environment*, *335*, 107995. https://doi.org/10.1016/j.agee.2022.107995

Yang, P., Wang, M. H., Lai, D. Y. F., Chun, K. P., Huang, J. F., Wan, S. A., et al. (2019). Methane dynamics in an estuarine brackish *Cyperus malaccensis* marsh: Production and porewater concentration in soils, and net emissions to the atmosphere over five years. *Geoderma*, *337*, 132–142. https://doi.org/10.1016/j.geoderma.2018.09.019

Yang, R. M., & Chen, L. M. (2020). *Spartina alterniflora* invasion alters soil bulk density in coastal wetlands of China. *Land Degradation & Development*, *32*, 1993–1999. https://doi.org/10.1002/ldr.3859

Yang, W., An, S. Q., Zhao, H., Xu, L. Q., Qiao, Y. J., & Cheng, X. L. (2016). Impacts of *Spartina alterniflora* invasion on soil organic carbon and nitrogen pools sizes, stability, and turnover in a coastal salt marsh of eastern China. *Ecological Engineering*, *86*, 174–182. https://doi.org/10.1016/j.ecoleng.2015.11.010

Yang, W., Zhao, H., Chen, X. L., Yin, S. L., Cheng, X. L., & An, S. Q. (2013). Consequences of short-term C_4 plant *Spartina alterniflora* invasions for soil organic carbon dynamics in a coastal wetland of Eastern China. *Ecological Engineering*, *61*, 50–57. https://doi.org/10.1016/j.ecoleng.2013.09.056

Ye, R., Jin, Q., Bohannan, B., Keller, J. K., McAllister, S. A., & Bridgham, S. D. (2012). pH controls over anaerobic carbon mineralization, the efficiency of methane production, and methanogenic pathways in peatlands across an ombrotrophic-minerotrophic gradient. *Soil Biology & Biochemistry*, *54*, 36–47. https://doi.org/10.1016/j.soilbio.2012.05.015

Yin, G. Y., Hou, L. J., Liu, M., Li, X. F., Zheng, Y. L., Gao, J., et al. (2017). DNRA in intertidal sediments of the Yangtze Estuary. *Journal of Geophysical Research: Biogeosciences*, *122*(8), 1988–1998. https://doi.org/10.1002/2017JG003766

Yin, S., Bai, J. H., Wang, W., Zhang, G. L., Jia, J., Cui, B. S., et al. (2019). Effects of soil moisture on carbon mineralization in floodplain wetlands with different flooding frequencies. *Journal of Hydrology*, *574*, 1074–1084. https://doi.org/10.1016/j.jhydrol.2019.05.007

Yuan, J. J., Liu, D. Y., Ji, Y., Xiang, J., Lin, Y. X., Wu, M., et al. (2019). *Spartina alterniflora* invasion drastically increases methane production potential by shifting methanogenesis from hydrogenotrophic to methylotrophic pathway in a coastal marsh. *Journal of Ecology*, *107*, 2436–2450. https://doi.org/10.1111/1365-2745.13164

Zhang, G. L., Bai, J. H., Zhao, Q. Q., Jia, J., Wang, X., Wang, W., et al. (2021a). Soil carbon storage and carbon sources under different *Spartina alterniflora* invasion periods in a salt marsh ecosystem. *Catena*, *196*, 104831. https://doi.org/10.1016/j.catena.2020.104831

Zhang, W. S., Li, H. P., Xiao, Q. T., & Li, X. Y. (2021c). Urban rivers are hotspots of riverine greenhouse gas (N_2O, CH_4, CO_2) emissions in the mixed-landscape chaohu lake basin. *Water Research*, *189*, 116624. https://doi.org/10.1016/j.watres.2020.116624

Zhang, X. M., Zhang, Z. S., Li, Z., Li, M., Wu, H. T., & Jiang, M. (2021b). Impacts of Spartina alterniflora invasion on soil carbon contents and stability in the Yellow River Delta, China. *Science of the Total Environment*, *775*, 145188. https://doi.org/10.1016/j.scitotenv.2021.145188

Zhang, Y. H., Ding, W. X., Luo, J. F., & Donnison, A. (2010). Changes in soil organic carbon dynamics in an Eastern Chinese coastal wetland following invasion by a C_4 plant *Spartina alterniflora*. *Soil Biology & Biochemistry*, *42*, 1712–1720. https://doi.org/10.1016/j.soilbio.2010.06.006

Zhu, Y. S., Wang, Y. D., Guo, C. C., Xue, D. M., Li, J., Chen, Q., et al. (2020). Conversion of coastal marshes to croplands decreases organic carbon but increases inorganic carbon in saline soils. *Land Degradation & Development*, *31*, 1099–1109. https://doi.org/10.1002/ldr.3538

Zou, S. B., Gao, Q., Cheng, H. H., Ni, M., Xu, Q., Liu M., et al. (2022). Vertical distribution of bacterial, sulfate-reducing and sulfur-oxidizing bacterial communities in sediment cores from freshwater prawn (*Macrobrachium rosenbergii*) aquaculture pond. *Acta Microbiologica Sinica*, *62*(7), 2719–2734 (in Chinese). https://doi.org/10.13343/j.cnki.wsxb.20210690

Figure captions

Figure 1. Locations of the study areas and 21 sampling sites across the coastal regions in southeastern China. Three wetland habitat types were investigated including mud flat (MFs), *S. alterniflora* marshes (SAs) and aquaculture ponds (APs).

Figure 2. Surface soil physicochemical properties across the three wetland habitat types (mean + SE; n = 63). MFs, SAs and APs represent mud flats, *S. alterniflora* marshes and aquaculture ponds, respectively. Different letters above the bars indicate significant differences (p<0.05).

Figure 3. Box plots of CO_2 and CH_4 production rates in surface soil for the three wetland habitat types, measured by incubation experiments (n = 63). MFs, SAs and APs represent mud flats, *S. alterniflora* marshes and aquaculture ponds, respectively. Different letters above the boxes indicate significant differences (p < 0.05).

Figure 4. (a) SOC mineralization rate in surface soil for the three wetland habitat types, measured by incubation experiments (mean ± SE; n = 63). (b) Boxplots of SOC mineralization rates for the three wetland habitat types; different letters above the boxes indicate significant differences (p < 0.05). MFs, SAs and APs represent mud flats, *S. alterniflora* marshes and aquaculture ponds, respectively.

Figure 5. (a) Cumulative SOC mineralization in surface soil over the 60-d incubation period for the three wetland habitat types (mean ± SE; n = 63). (b) Boxplots of cumulative SOC mineralization for the three wetland habitat types; different letters above the bars indicate significant differences (p < 0.05). MFs, SAs and APs represent mud flats, *S. alterniflora* marshes and aquaculture ponds, respectively.

Figure 6. Weighted response ratios (RR_{++}) of (a) SOC mineralization rate, (b) cumulative SOC mineralization (ΣSOCM), (c) initial SOC (C_0) and (d) mineralization rate constant (k) for the different habitat modification scenarios: MFs → SAs represents conversion of mudflats to *S. alterniflora* marshes; SAs → APs represents conversion of *S. alterniflora* marshes to aquaculture ponds. Bars represent the RR++ values and 95% CIs (n = 63). Effects of habitat modifications were significant at p < 0.05 in all cases.

Figure 7. Redundancy analysis (RDA) biplots of the relationship between $\Delta\Sigma$SOCM, ΔC_0, Δk, and $\Delta(C_0/SOC)$, and ΔEF (environment factors) for the different habitat modification scenarios: (a) conversion of mud flats to *S. alterniflora* marshes; (b) conversion of *S. alterniflora* marshes to aquaculture ponds. The pie charts show the percentages of variance in $\Delta\Sigma$SOCM explained by the different variables. List of abbreviations is provided in the text.

Figure 8. A schematic illustration of landscape change effects on soil organic carbon mineralization and carbon emission in impacted coastal wetlands across a wide latitudinal range in China.

Figure 9. Changes in coastal landscape and related soil CO_2-eq production in China: (a) *S. alterniflora* marsh area (from Mao et al., 2019), estimated marsh soil CO_2-eq production and net increase relative to native mudflats; (b) coastal aquaculture pond area (from Duan et al., 2021), estimated pond soil CO_2-eq production and net increase relative to native mudflats. See text (section 4.4) for explanation.

Table 1

Fitting parameters of the first order kinetics and C_0/SOC values for SOC mineralization in surface soil (0–20 cm) across the three wetland habitat types.

Habitat types	**$\Sigma SOCM_{final}$ (μg g^{-1})**	**Fitting parameters**			**$\Sigma SOCM_{final}/C_0$**	**C_0/SOC**
		C_0 (μg g^{-1})	**k (d^{-1})**	**Adj. R^2**		
Mud flat	95.0	88.8	0.127	0.94	1.07	0.013
***S. alterniflora* marshes**	162.9	152.3	0.127	0.95	1.07	0.016
Aquaculture ponds	135.0	125.6	0.126	0.95	1.08	0.015

Table 2

Pearson correlation coefficients between changes in ΣSOCM, C_0, k and C_0/SOC, and different environmental variables in surface soil (0–20 cm) for the different habitat change scenarios: conversion of mudflat to *S. alterniflora* marshes, and conversion of *S. alterniflora* marshes to aquaculture ponds. SOC, MBC and MBN represent soil organic carbon, microbial biomass carbon and microbial biomass nitrogen, respectively. Significant correlations are indicated by the symbols * ($p < 0.05$) and ** ($p < 0.01$).

Environmental variables	Conversion of mud flat to *S. alterniflora* marshes				Conversion of *S. alterniflora* marshes to aquaculture ponds			
	ΔΣSOCM	ΔC_0	Δk	$\Delta C_0/SOC$	ΔΣSOCM	ΔC_0	Δk	$\Delta C_0/SOC$
pH	-0.165	-0.155	0.021	**-0.259****	**-0.342****	**-0.344****	0.004	-0.037
Soil salinity	-0.036	-0.024	-0.171	**-0.377****	-0.144	-0.139	**-0.246****	**-0.261****
Soil water content	0.139	0.147	-0.030	**-0.254****	-0.084	-0.072	0.061	**-0.296****
Soil bulk density	**-0.285****	**-0.293****	-0.053	**0.176***	-0.137	-0.144	-0.089	0.148
NH_4^+-N	**0.441****	**0.451****	-0.034	-0.029	**0.536****	**0.547****	0.147	-0.225
NO_3^--N	0.057	0.061	0.039	-0.133	-0.077	-0.082	-0.100	0.068
Soil C:N	-0.114	-0.131	-0.118	**0.253****	-0.146	-0.158	0.056	**0.262****
Cl^-	-0.024	-0.020	**-0.208***	-0.115	-0.133	-0.130	**-0.301****	**-0.208***
SO_4^{2-}	0.034	0.034	-0.062	-0.076	0.058	0.057	-0.146	-0.025
SOC	**0.739****	**0.739****	-0.132	**0.193***	**0.795****	**0.800****	-0.125	0.162
MBC	**0.401****	**0.393****	0.120	0.072	**0.458****	**0.450****	-0.128	0.155
MBN	**0.300****	**0.305****	-0.122	0.002	**0.389****	**0.397****	-0.014	-0.063
Soil clay content	**0.248****	**0.252****	0.098	-0.107	**0.334****	**0.340****	0.102	-0.109
Soil silt content	0.114	0.119	-0.013	-0.139	0.152	0.159	0.141	-0.131
Soil sandy content	-0.139	-0.144	-0.006	0.136	**-0.187***	**-0.194***	-0.136	0.129

Table 3

Habitat Ratio for SOC, C_0 and ΣSOCM, based on data from Fig. 2 and Table 1. MFs, SAs and APs represent mud flats, *S. alterniflora* marshes and aquaculture ponds, respectively.

	SAs : APs : MFs
SOC	1.50 : 1.25 : 1
$\boldsymbol{C_0}$	1.72 : 1.41 : 1
ΣSOCM	1.71 : 1.42 : 1

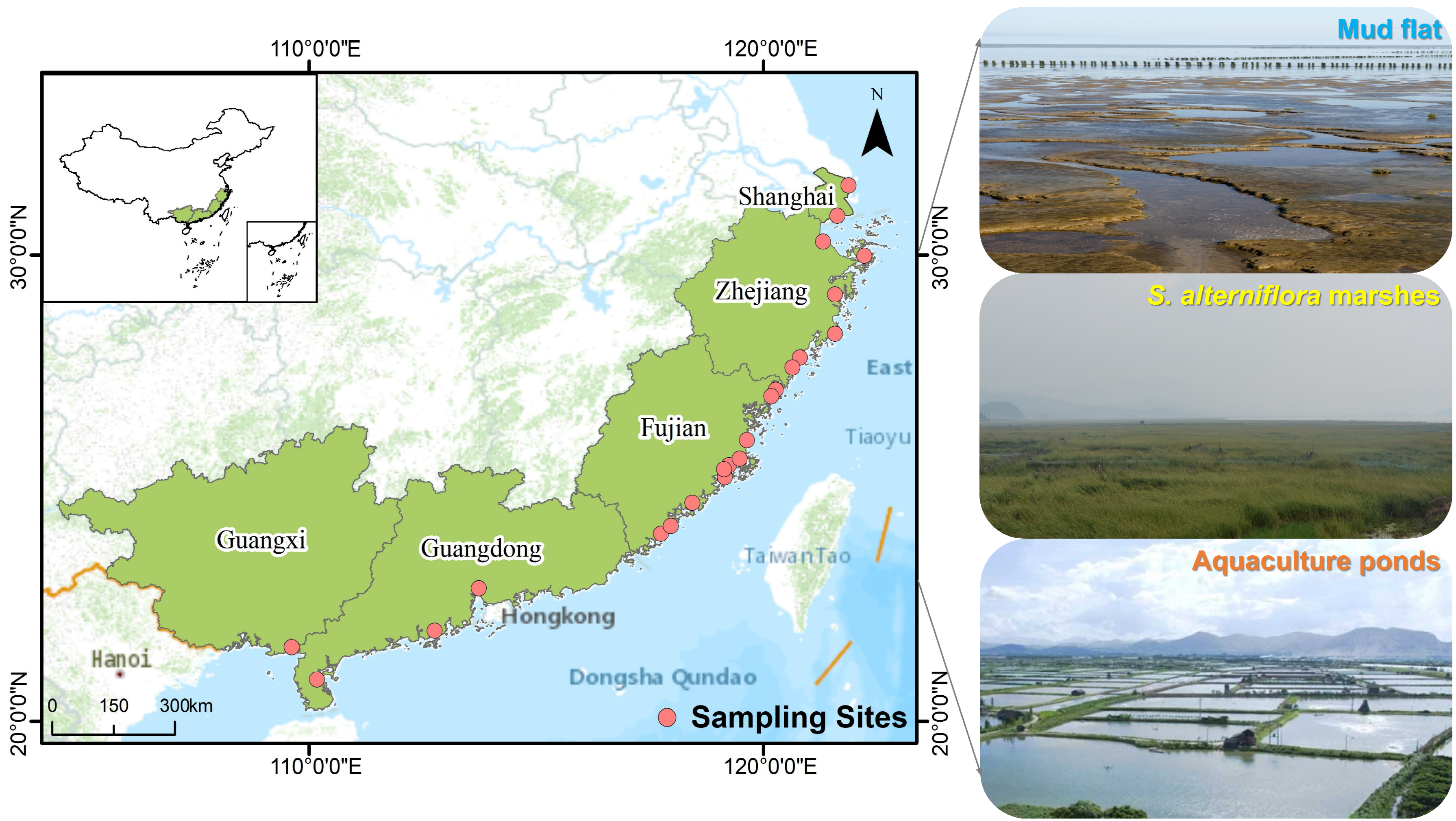

Figure 1. Locations of the study areas and 21 sampling sites across the coastal regions in southeastern China. Three wetland habitat types were investigated including mud flat (MFs), *S. alterniflora* marshes (SAs) and aquaculture ponds (APs).

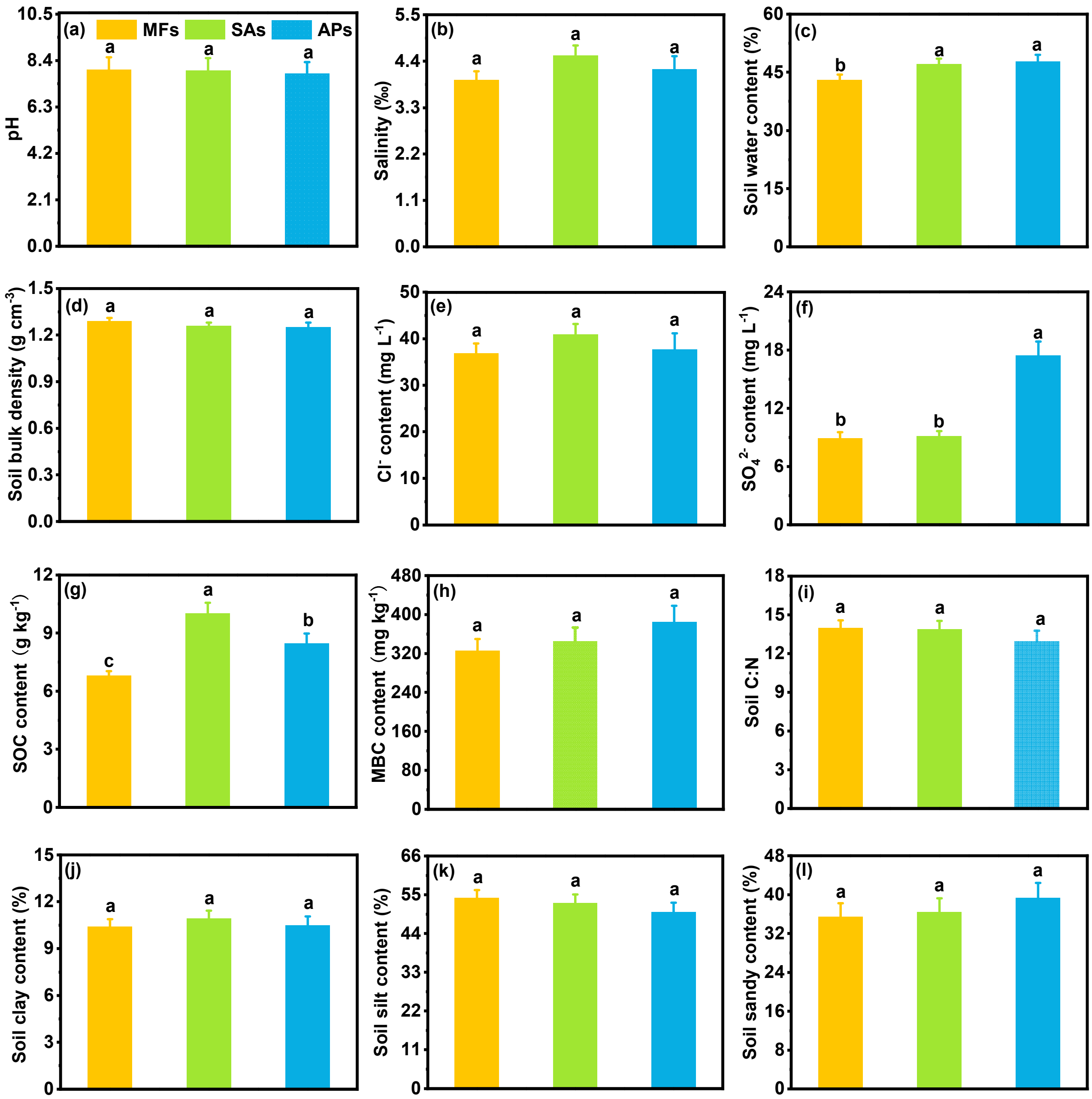

Figure 2. Surface soil physicochemical properties across the three wetland habitat types (mean + SE; $n = 63$). MFs, SAs and APs represent mud flats, *S. alterniflora* marshes and aquaculture ponds, respectively. Different letters above the bars indicate significant differences ($p<0.05$).

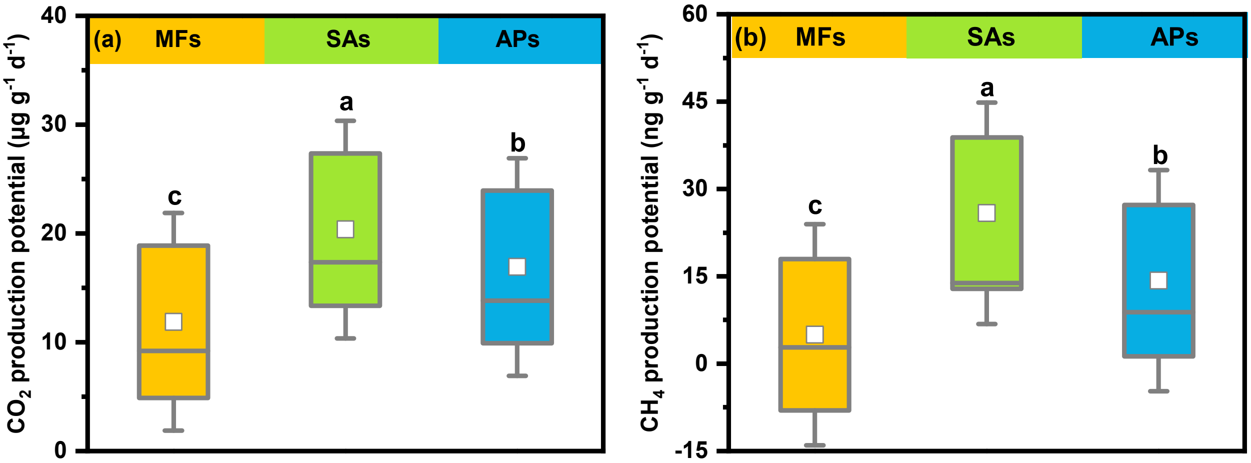

Figure 3. Box plots of CO_2 and CH_4 production rates in surface soil for the three wetland habitat types, measured by incubation experiments (n = 63). MFs, SAs and APs represent mud flats, *S. alterniflora* marshes and aquaculture ponds, respectively. Different letters above the boxes indicate significant differences ($p < 0.05$).

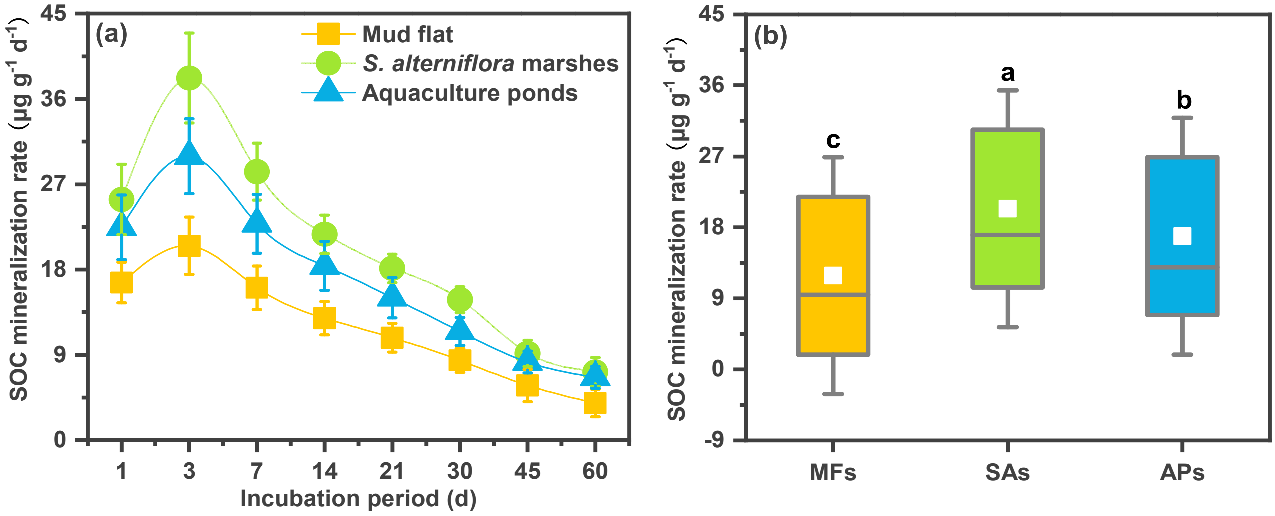

Figure 4. (a) SOC mineralization rate in surface soil for the three wetland habitat types, measured by incubation experiments (mean ± SE; n = 63). (b) Boxplots of SOC mineralization rates for the three wetland habitat types; different letters above the boxes indicate significant differences (p < 0.05). MFs, SAs and APs represent mud flats, *S. alterniflora* marshes and aquaculture ponds, respectively.

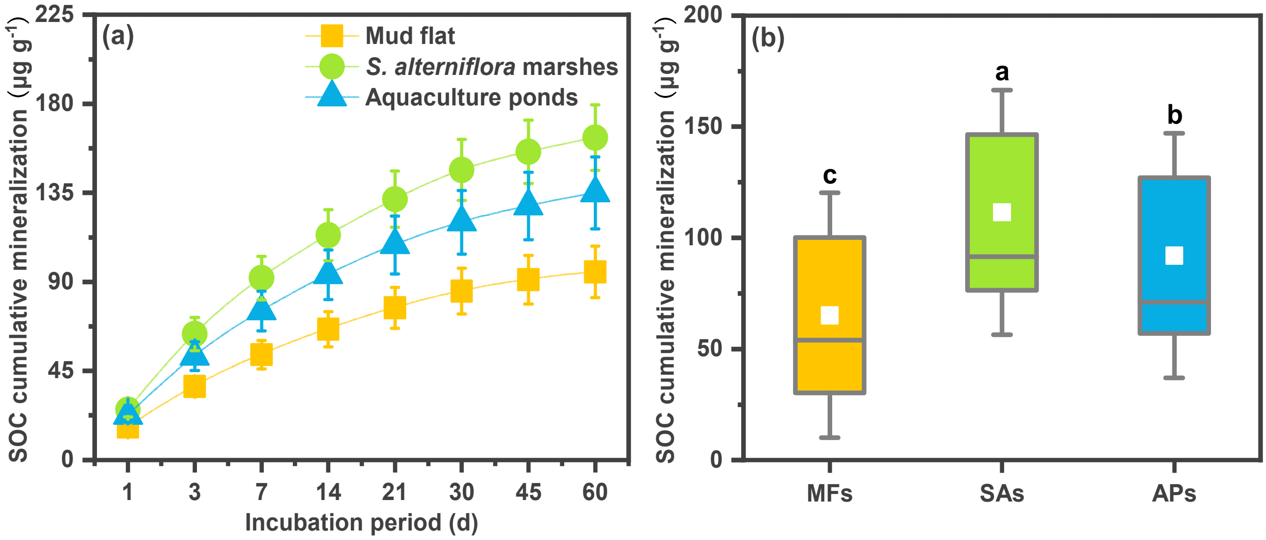

Figure 5. (a) Cumulative SOC mineralization in surface soil over the 60-d incubation period for the three wetland habitat types (mean ± SE; n = 63). (b) Boxplots of cumulative SOC mineralization for the three wetland habitat types; different letters above the bars indicate significant differences ($p < 0.05$). MFs, SAs and APs represent mud flats, *S. alterniflora* marshes and aquaculture ponds, respectively.

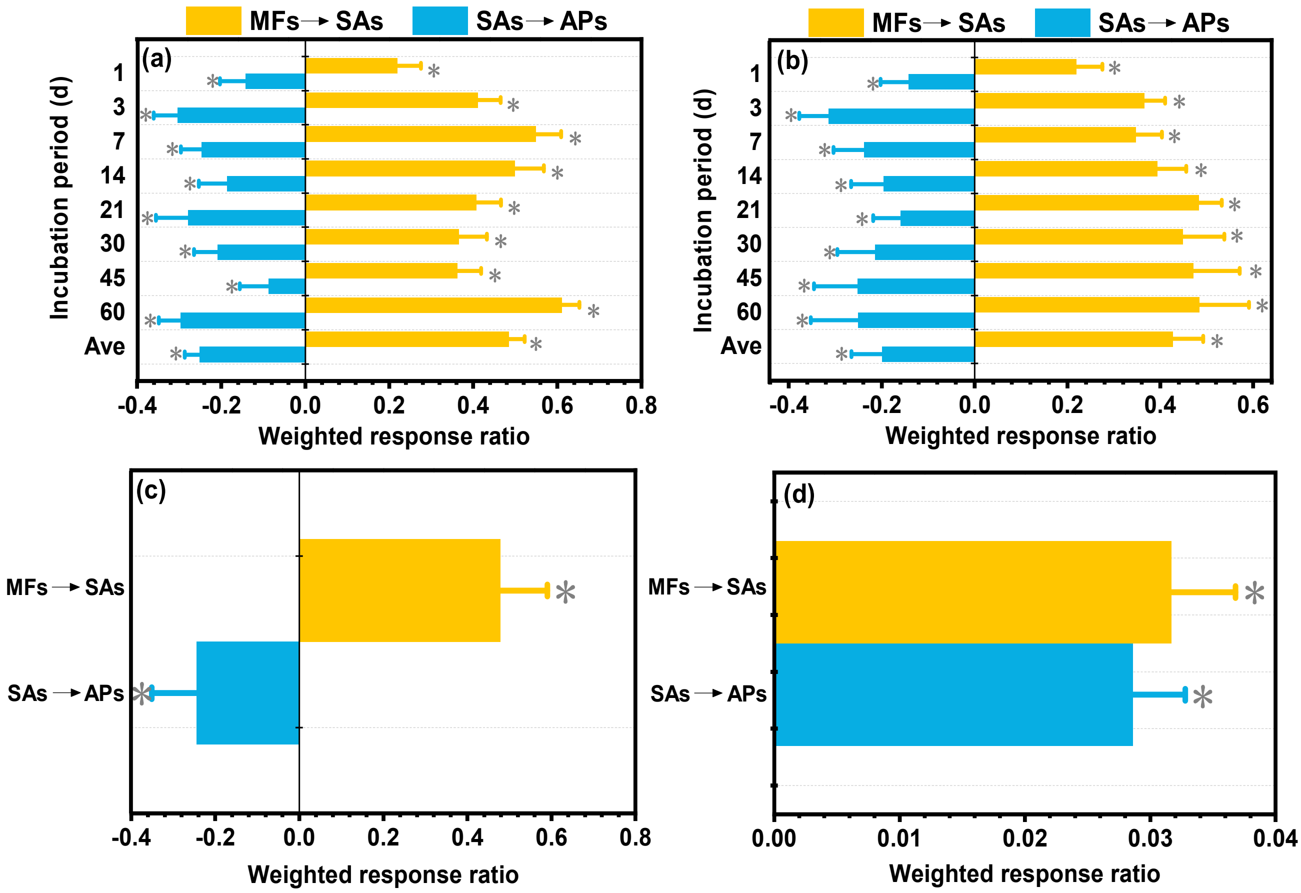

Figure 6. Weighted response ratios (RR_{++}) of (a) SOC mineralization rate, (b) cumulative SOC mineralization (ΣSOCM), (c) initial SOC (C_0) and (d) mineralization rate constant (k) for the different habitat modification scenarios: MFs → SAs represents conversion of mudflats to *S. alterniflora* marshes; SAs → APs represents conversion of *S. alterniflora* marshes to aquaculture ponds. Bars represent the RR++ values and 95% CIs (n = 63). Effects of habitat modifications were significant at $p < 0.05$ in all cases.

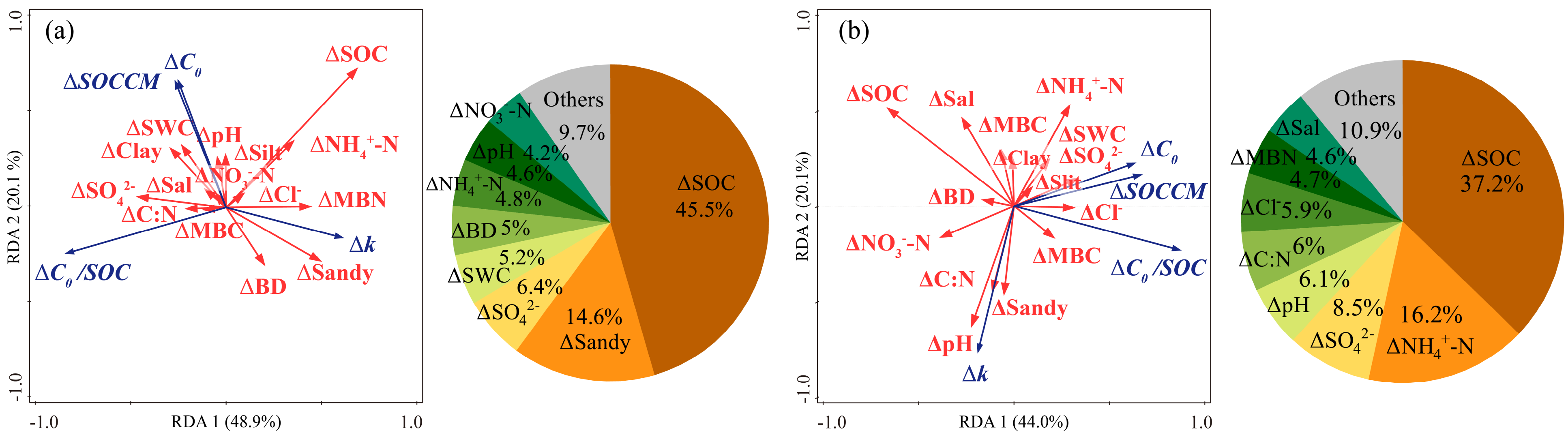

Figure 7. Redundancy analysis (RDA) biplots of the relationship between ΔΣSOCM, ΔC_0, Δk, and $\Delta(C_0/SOC)$, and ΔEF (environment factors) for the different habitat modification scenarios: (a) conversion of mud flats to *S. alterniflora* marshes; (b) conversion of *S. alterniflora* marshes to aquaculture ponds. The pie charts show the percentages of variance in ΔΣSOCM explained by the different variables. List of abbreviations is provided in the text.

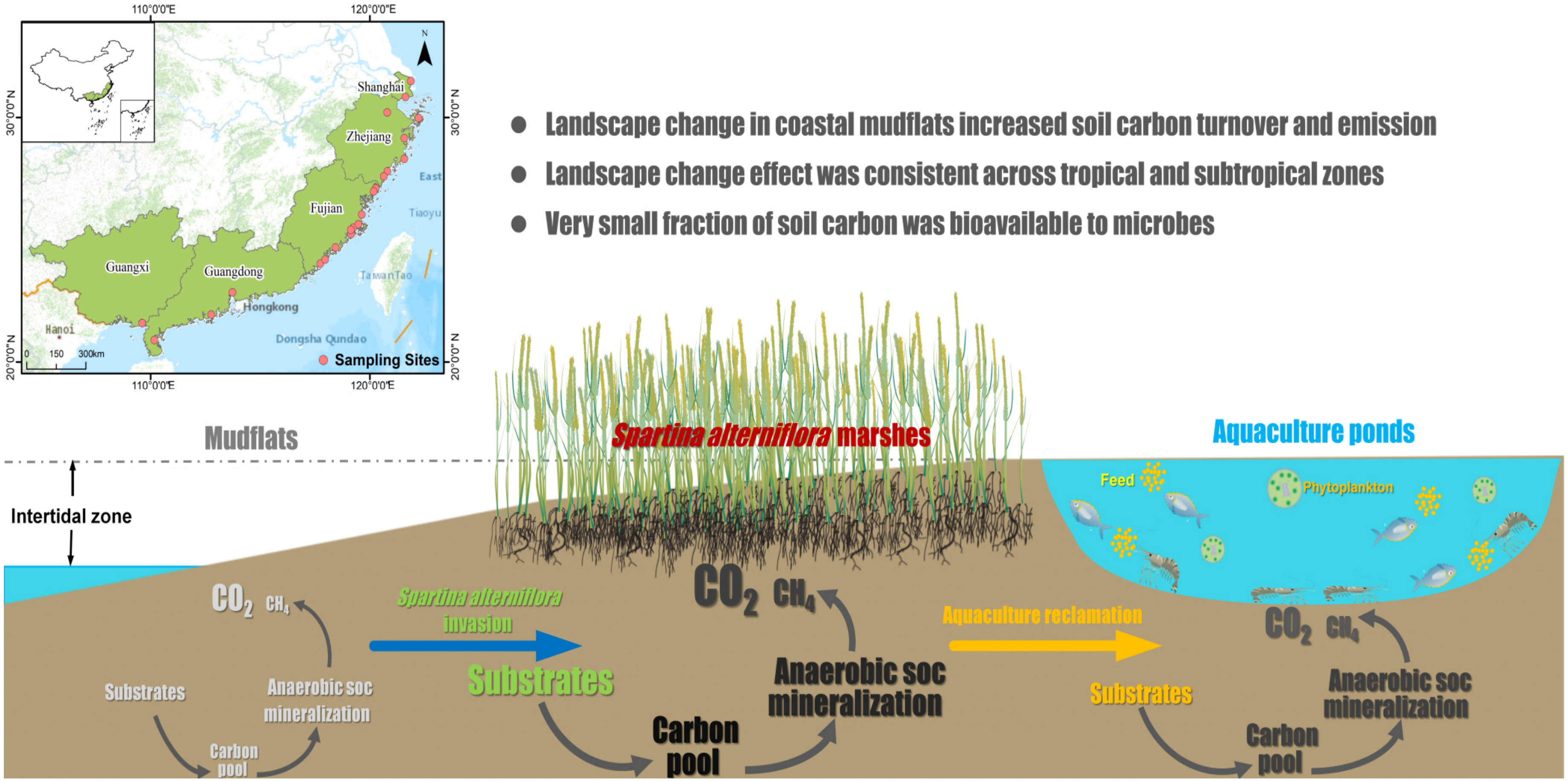

Figure 8. A schematic illustration of landscape change effects on soil organic carbon mineralization and carbon emission in impacted coastal wetlands across a wide latitudinal range in China.

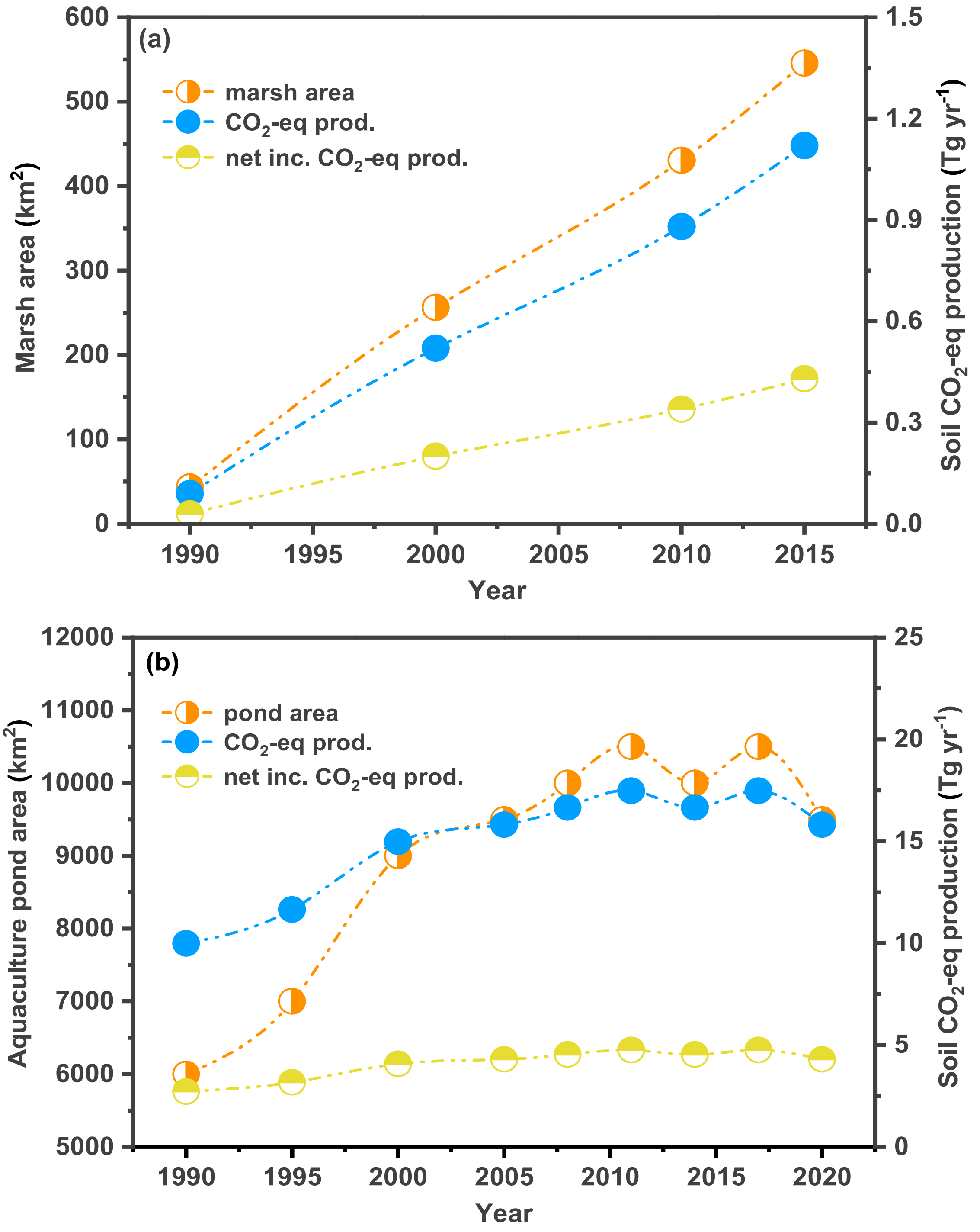

Figure 9. Changes in coastal landscape and related soil CO_2-eq production in China: (a) *S. alterniflora* marsh area (from Mao et al., 2019), estimated marsh soil CO_2-eq production and net increase relative to native mudflats; (b) coastal aquaculture pond area (from Duan et al., 2021), estimated pond soil CO_2-eq production and net increase relative to native mudflats. See text (section 4.4) for explanation.

Supporting Information

Landscape Change Affects Soil Organic Carbon Mineralization and Greenhouse Gas Production in Coastal Wetlands

Ping Yang[1,2,3*], Linhai Zhang[1,2,3], Derrick Y. F. Lai[4], Hong Yang[5,6], Lishan Tan[7], Liangjuan Luo[1,2], Chuan Tong[1,2,3*], Yan Hong[1,2], Wanyi Zhu[1,2], Kam W. Tang[8*]

[1]*School of Geographical Sciences, Fujian Normal University, Fuzhou 350007, P.R. China,*

[2]*Key Laboratory of Humid Subtropical Eco-geographical Process of Ministry of Education, Fujian Normal University, Fuzhou 350007, P.R. China*

[3]*Research Centre of Wetlands in Subtropical Region, Fujian Normal University, Fuzhou 350007, P.R. China*

[4]*Department of Geography and Resource Management, The Chinese University of Hong Kong, Shatin, New Territories, Hong Kong SAR 999077, China*

[5]*State Key Laboratory of Estuarine and Coastal Research, East China Normal University, Shanghai 200241, China*

[6]*College of Environmental Science and Engineering, Fujian Normal University, Fuzhou 350007, China*

[7]*Department of Geography and Environmental Science, University of Reading, Reading RG6 6AB, U.K.*

[8]*Department of Biosciences, Swansea University, Swansea SA2 8PP, U.K.*

***Correspondence to:**

Ping Yang (yangping528@sina.cn); Chuan Tong (tongch@fjnu.edu.cn); Kam W. Tang (k.w.tang@swansea.ac.uk)

Supporting Information Summary

No. of pages: 3 No. of tables: 1

Page S3: Table S1. Fitting parameters of the first order kinetics for soil organic carbon mineralization in surface soil (0–20 cm) from three wetland habitat types across the different coastal sites in China.

Table S1.

Fitting parameters of the first order kinetics for soil organic carbon mineralization in surface soil (0–20 cm) from three wetland habitat types across different coastal sites in China.

Province	Site	Mud flat				*S. alterniflora* marshes				Aquaculture ponds			
		C_t (μg g^{-1})	C_0 (μg g^{-1})	k (d^{-1})	Adj. R^2	C_t (μg g^{-1})	C_0 (μg g^{-1})	k (d^{-1})	Adj. R^2	C_t (μg g^{-1})	C_0 (μg g^{-1})	k (d^{-1})	Adj. R^2
Shanghai	Chongming Island	59.708	59.708	0.234	0.842	96.641	96.653	0.150	0.901	68.720	68.724	0.163	0.896
	Fengxian	88.107	88.143	0.130	0.907	191.760	191.794	0.144	0.905	93.598	93.763	0.106	0.939
Zhejiang	Hangzhou Gulf	51.653	51.655	0.166	0.874	116.563	116.666	0.117	0.942	82.363	82.394	0.131	0.932
	Zhoushan	48.190	48.191	0.185	0.875	162.268	162.359	0.125	0.932	120.336	120.345	0.157	0.876
	Ningbo	55.554	55.554	0.265	0.841	178.106	178.200	0.126	0.959	132.292	132.293	0.187	0.880
	Taizhou	134.553	134.612	0.129	0.952	160.502	160.715	0.110	0.953	111.661	111.668	0.160	0.942
	Dragon Bay	91.719	91.846	0.110	0.945	134.200	134.234	0.138	0.947	103.386	103.386	0.219	0.893
	Aojiang River estuary	85.142	85.391	0.097	0.978	133.976	134.643	0.088	0.984	116.388	116.585	0.106	0.970
Fujian	Chatanggang	85.309	85.384	0.117	0.969	164.445	165.903	0.079	0.987	132.004	132.621	0.090	0.985
	Yacheng	86.954	87.020	0.120	0.966	113.018	113.270	0.102	0.981	103.682	103.813	0.111	0.963
	Min River estuary	239.225	239.461	0.115	0.951	256.076	256.077	0.213	0.919	270.811	271.297	0.105	0.958
	Xinghua Bay	51.967	51.994	0.126	0.922	165.279	165.468	0.113	0.924	89.684	89.698	0.146	0.883
	Fuqing Bay	67.353	67.434	0.112	0.984	87.516	87.744	0.099	0.976	67.808	67.827	0.136	0.980
	Shangwuyu	63.289	63.387	0.108	0.974	121.368	122.564	0.077	0.989	74.173	74.336	0.102	0.983
	Mulanxi	77.767	77.817	0.122	0.981	130.130	130.895	0.086	0.984	93.042	93.209	0.105	0.976
	Jiuzhengang	68.288	68.417	0.105	0.956	91.379	91.402	0.138	0.958	83.658	83.722	0.120	0.962
	Chiyugang	69.104	69.142	0.125	0.959	86.432	86.454	0.138	0.962	80.699	80.780	0.115	0.978
Guangdong	Shijing River estuary	51.101	51.224	0.101	0.963	80.218	80.237	0.139	0.959	82.406	82.512	0.111	0.972
	Guanghai	252.227	252.312	0.133	0.935	373.120	373.155	0.155	0.950	365.538	365.660	0.133	0.941
	Leidong Peninsula	75.914	75.926	0.146	0.941	250.627	250.633	0.178	0.952	269.499	269.588	0.134	0.943
Guangxi	Beibu Gulf	61.354	61.354	0.205	0.857	112.097	112.127	0.137	0.909	95.842	95.865	0.139	0.903

Supporting Information

Landscape Change Affects Soil Organic Carbon Mineralization and Greenhouse Gas Production in Coastal Wetlands

Ping Yang[1,2,3*], Linhai Zhang[1,2,3], Derrick Y. F. Lai[4], Hong Yang[5,6], Lishan Tan[7], Liangjuan Luo[1,2], Chuan Tong[1,2,3*], Yan Hong[1,2], Wanyi Zhu[1,2], Kam W. Tang[8*]

[1]*School of Geographical Sciences, Fujian Normal University, Fuzhou 350007, P.R. China,*

[2]*Key Laboratory of Humid Subtropical Eco-geographical Process of Ministry of Education, Fujian Normal University, Fuzhou 350007, P.R. China*

[3]*Research Centre of Wetlands in Subtropical Region, Fujian Normal University, Fuzhou 350007, P.R. China*

[4]*Department of Geography and Resource Management, The Chinese University of Hong Kong, Shatin, New Territories, Hong Kong SAR 999077, China*

[5]*State Key Laboratory of Estuarine and Coastal Research, East China Normal University, Shanghai 200241, China*

[6]*College of Environmental Science and Engineering, Fujian Normal University, Fuzhou 350007, China*

[7]*Department of Geography and Environmental Science, University of Reading, Reading RG6 6AB, U.K.*

[8]*Department of Biosciences, Swansea University, Swansea SA2 8PP, U.K.*

***Correspondence to:**

Ping Yang (yangping528@sina.cn); Chuan Tong (tongch@fjnu.edu.cn); Kam W. Tang (k.w.tang@swansea.ac.uk)

Supporting Information Summary

No. of pages: 4   No. of figures: 2

Page S3: Figure S1. Soil organic carbon mineralization rate in surface soil (0–20 cm) from three wetland habitat types across the different coastal sites in China.

Page S4: Figure S2. Cumulative mineralization of soil organic carbon in surface soil (0–20 cm) from three wetland habitat types across the different coastal sites in China.

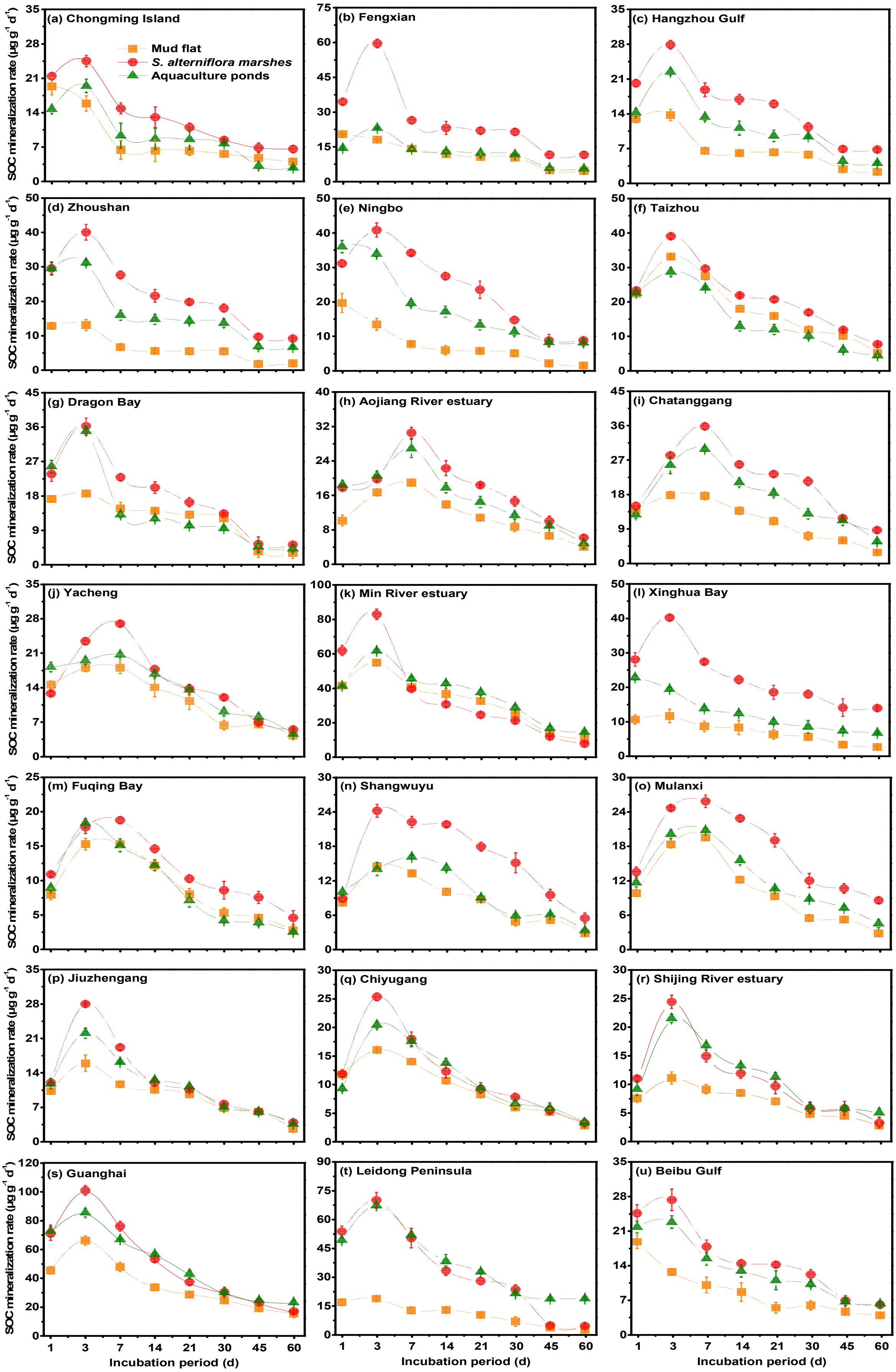

Figure S1. Soil organic carbon mineralization rates in surface soil (0–20 cm) from three wetland habitat types across different coastal sites in China.

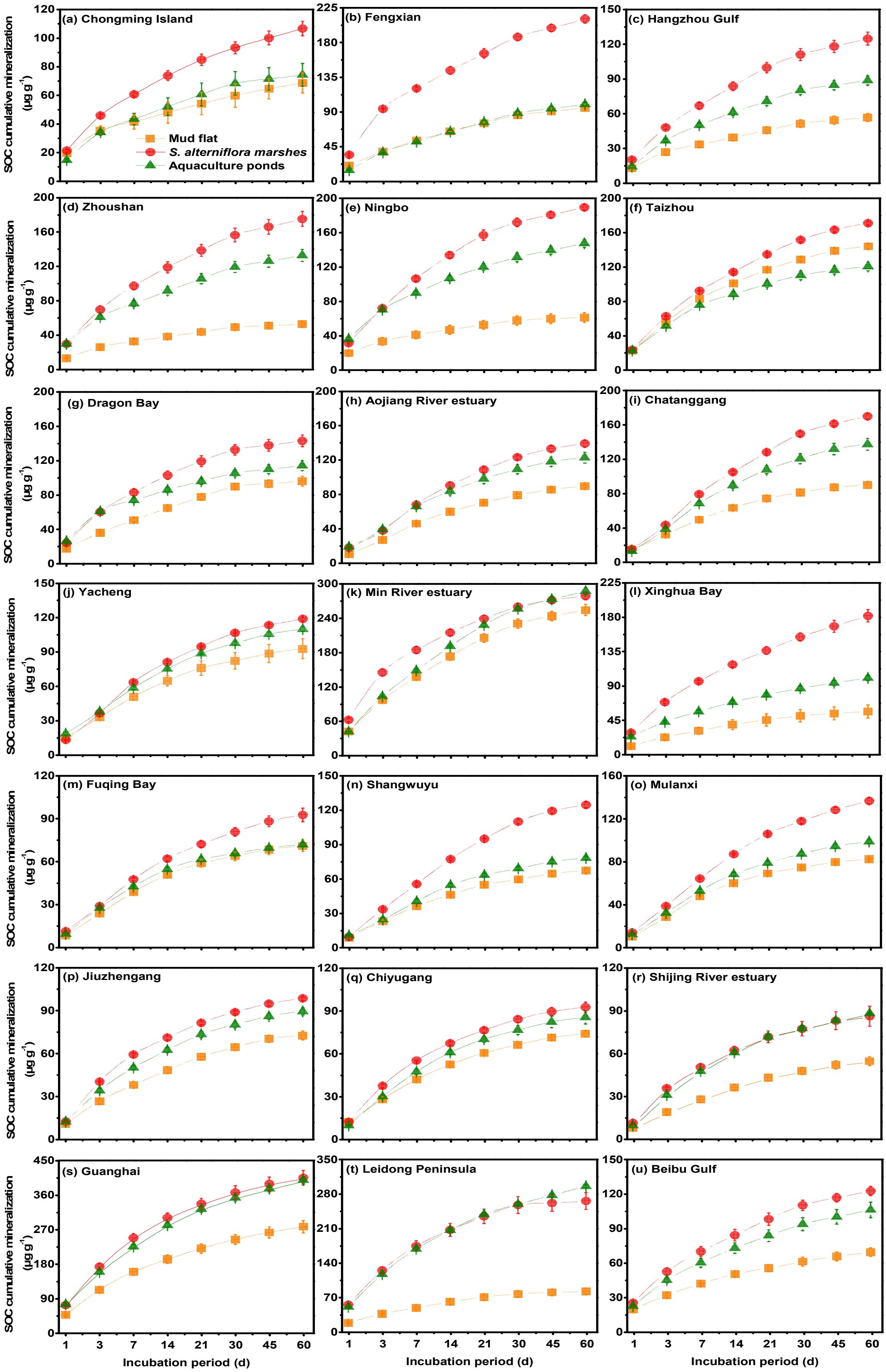

Figure S2. Cumulative mineralization of soil organic carbon in surface soil (0–20 cm) from three wetland habitat types across different coastal sites in China.